Eco-morphodynamics of coastal wetlands

Nicoletta Tambroni[1] · Stefano Lanzoni[2] · Giovanni Seminara[1]

Abstract

We survey the problem of the response of coastal wetlands to sea level rise. Two opposite views have traditionally been confronted. According to the former, on the geological time scale, coastal lagoons would be 'ephemeral' features. The latter view maintains that marshes would keep pace with relative sea level rise as, increasing the rate of the latter, the sedimentation rate would also increase. In any case, the timescale of morphodynamic evolution is of the order of centuries, which makes it not easily perceived. For example, in Venice, the diversion of the rivers debouching into the lagoon undertaken in the Renaissance has taken centuries to display its consequences (shift from depositional to erosional environment). This process accelerated in the last two centuries due to effects of the industrial revolution and of an enhanced sea level rise. Recent research has employed powerful computational techniques and advanced models of marsh vegetation. Zero-order modeling suggests that marsh equilibrium is possible, provided the rate of relative sea level rise does not exceed a threshold depending on the availability of minerogenic sediments, quantified through a loosely defined ambient sediment concentration. Analysis of the morphological interaction between adjacent morphological units suggests that the 'equilibrium states' identified by zero-order modeling correspond to marshes which either prograde or retreat, i.e., are not in equilibrium. Results suggest that available techniques, e.g., artificial replenishment of salt marshes or search for more productive halophytic species, will hardly allow Venice wetlands to keep up with a strong acceleration of sea level rise.

Keywords Coastal wetlands · Eco-morphodynamics · Sea level rise · Morphological equilibrium · Tidal environments

✉ Nicoletta Tambroni
nicoletta.tambroni@unige.it

Stefano Lanzoni
stefano.lanzoni@unipd.it

Giovanni Seminara
giovanni.seminara@unige.it

[1] Department of Civil, Chemical and Environmental Engineering, Università di Genova, Via Montallegro 1, 16145 Genova, Italy

[2] Department of Civil, Environmental and Architectural Engineering, Università di Padova, Via Loredan 20, 35131 Padova, Italy

1 Introduction

One of the major expressions of climate change is an accelerated sea level rise (slr hereafter). Figure 1 shows projections reported in the latest IPCC Assessment Report (IPCC 2021). They show that we may expect changes in the mean sea level (m.s.l.) by 2100 relative to 1995–2014 in the ranges 0.28–1.01 m depending on the adopted Greenhouse Gas (GHG) emission scenario. Quoting Lambeck (2021): although "*the science of sea-level projections is still in its infancy .. we can have confidence in the general directions of the projections, albeit with less confidence in their rates*".

Even more threatening is the statement (to which IPCC attaches *high confidence*) that "*sea level is committed to rise for centuries to millennia due to continuing deep ocean warming and ice sheet melt, and will remain elevated for thousands of years*": with low confidence projections of 2–3 m rise over the next 2000 years if warming is limited to 1.5 °C and 2–6 m with 2 °C warming. The actual threat associated with the latter projections is subject to large uncertainty as it will depend strongly on the hardly predictable

Fig. 1 Projections of global mean sea level change (in m) relative to 1900 based on the various scenarios examined in IPCC (2021)
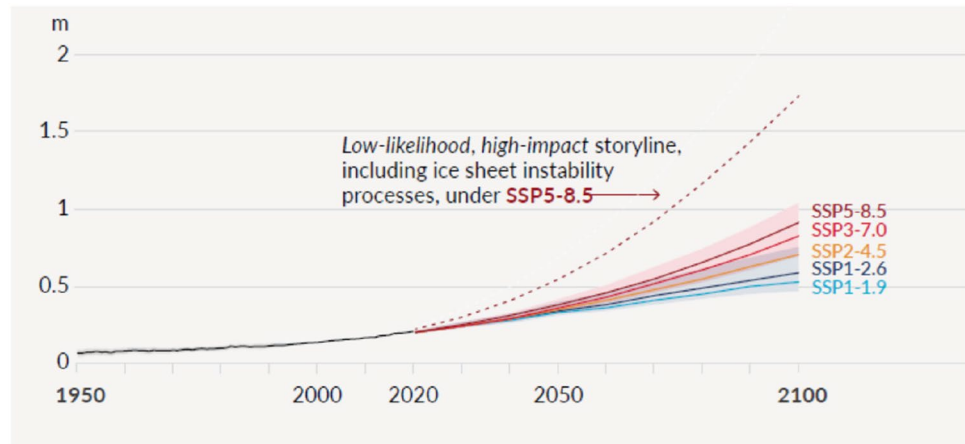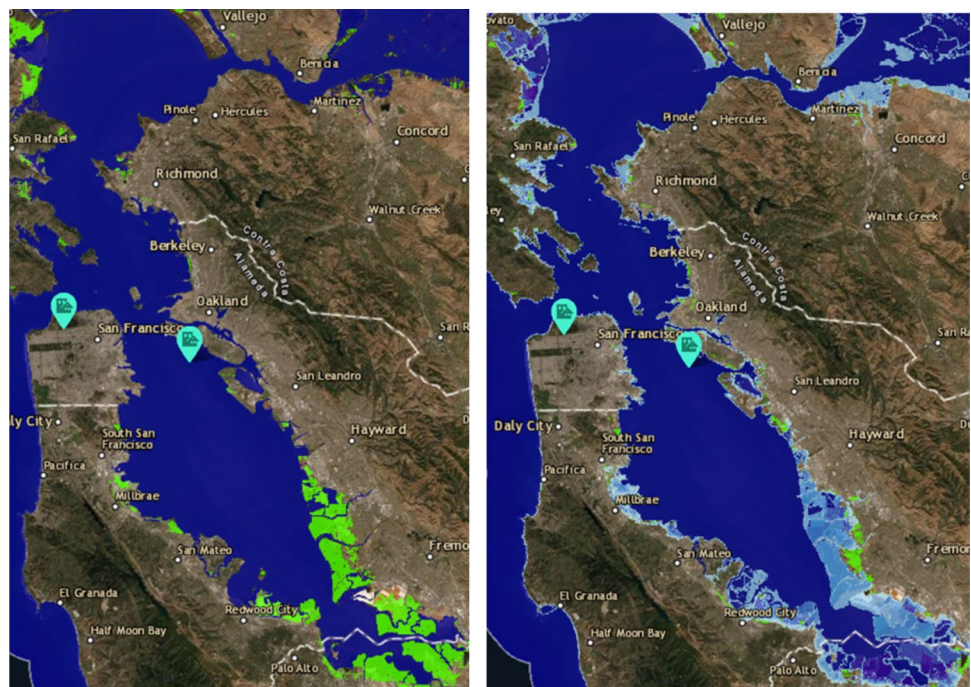

demographic evolution of the planet, as well as on the effectiveness of mitigation and adaptation policies which depend in turn on future technological developments. However, whatever action will be implemented, it will hardly be able to stop rapidly a process whose persistence is due to the enormous inertia of the natural system involved, namely the Earth hydrosphere, atmosphere and biosphere. Hence, the issue of how coastal regions will be affected by sea level rise in this century, is definitely on the table. This is admittedly an enormous problem as it involves some of the most populated areas of the world, namely low lying deltas.

Here, the effects of sea level rise are enhanced by further simultaneous factors, like natural and anthropogenic subsidence, combined with a decreased influx of fluvial sediments due to upstream river regulation works. The size of the threat for coastal communities was estimated long ago for the Nile and Bangladesh deltas by Milliman et al. (1989), who pointed out that, at the higher values of slr, Egypt and Bangladesh could lose 26 and 34% of their currently habitable land by 2100, respectively, and this would result in severe loss of their Gross Domestic Product. Nowadays, sea level rise maps, that allow users to visualize community-level impacts from coastal flooding or sea level rise, are available in some countries (e.g., NOAA's maps in USA). An instructive example is given in Fig. 2, which shows that, in the absence of appropriate countermeasures, a 0.9 m slr would be sufficient to drown all the remaining wetlands bordering San Francisco Bay,

Fig. 2 The picture shows the effect that a 0.9 m slr would have on the coast of the San Francisco Bay. Left: present, right: 0.9 m slr. Green: marshlands; light blue: drowned areas; brown: land (NOAA's Map Viewer. https://www.climate.gov/maps-data/dataset/sea-level-rise-map-viewer) (color figure online)

Rendiconti Lincei. Scienze Fisiche e Naturali (2022) 33:217–243

219

besides affecting a number of important settlements of the Silicon Valley.

Besides the loss of biodiversity and ecosystem services associated with wetland drowning, a major impact of slr is to increase vulnerability to inundation of low lying coastal areas as a result of deterioration of the natural defense opposed to coastal storms by barrier islands and wetlands (Day and Templet 1989). This may be clearly inferred from Fig. 3, that shows that, unless adaptation measures will be undertaken, a 0.9 m sea level rise would drown most of the Mississippi delta and all the barrier islands present along that reach of the coast of Louisiana.

However, the above pictures, suggestive as they may be, do not tell the whole story about the future of wetlands, as they do not account for the morphological variations that these features may undergo in the time span needed for sea level rise. Predicting this process poses a rather tough problem, that has been widely investigated in the last few decades but cannot be described as fully settled yet. Indeed, the crucial factor controlling the 'health' of wetlands is the exchange of water and sediments with the inland and the ocean and, in this respect, a wide spectrum of transitional environments are observed (Kjerfve 1994). They are significantly affected by the various types of hydrodynamic forcing, marine (tides and waves), fluvial and atmospheric (wind). The transitional waters may display a widely varying degree of salinity, ranging from brackish to saline. Tidally dominated environments, which are the subjects of the present review, comprise various distinct morphological units (Seminara et al. 2001): barrier islands, inlets, channels, shoals (also called sub-tidal flats, *bassifondi* in Venice), tidal flats (*velme* in Venice) and marshes (*barene* in Venice) (Fig. 4). The evolution of different morphological units is controlled by different dominant processes: wave attack and possibly aeolian transport affect barrier islands; wave resuspension in the surf zone, littoral currents and tidal currents control inlet morphodynamics; tide propagation is dominant in tidal channels; wind resuspension and tidal circulation operate in the shoals and tidal flats; the presence of halophytic vegetation, with the variety of biological and physical processes it determines, is the distinct feature of marshes.

The survival of these complex and delicate environments, which are sites of great biodiversity and significant economic value, is of great concern for the scientific community and poses a fundamental question: can a coastal lagoon reach an *equilibrium state*? In the present paper, we wish to review the available knowledge on this major issue, devoting special attention to the problem of ascertaining to what extent coastal lagoons may be able to survive an accelerated sea level rise. Note that the issue of morphodynamic equilibrium has enjoyed an increasing popularity in the last few decades (Zhou et al. 2017) and


Fig. 3 The picture shows the effect that a 0.9 m sea level rise would have on the coast of Louisiana, near New Orleans. Top: 0.9 m slr, bottom: present. Green: marshlands; light blue: drowned areas; brown: land (NOAA's Map Viewer. https://www.climate.gov/maps-data/dataset/sea-level-rise-map-viewer) (color figure online)
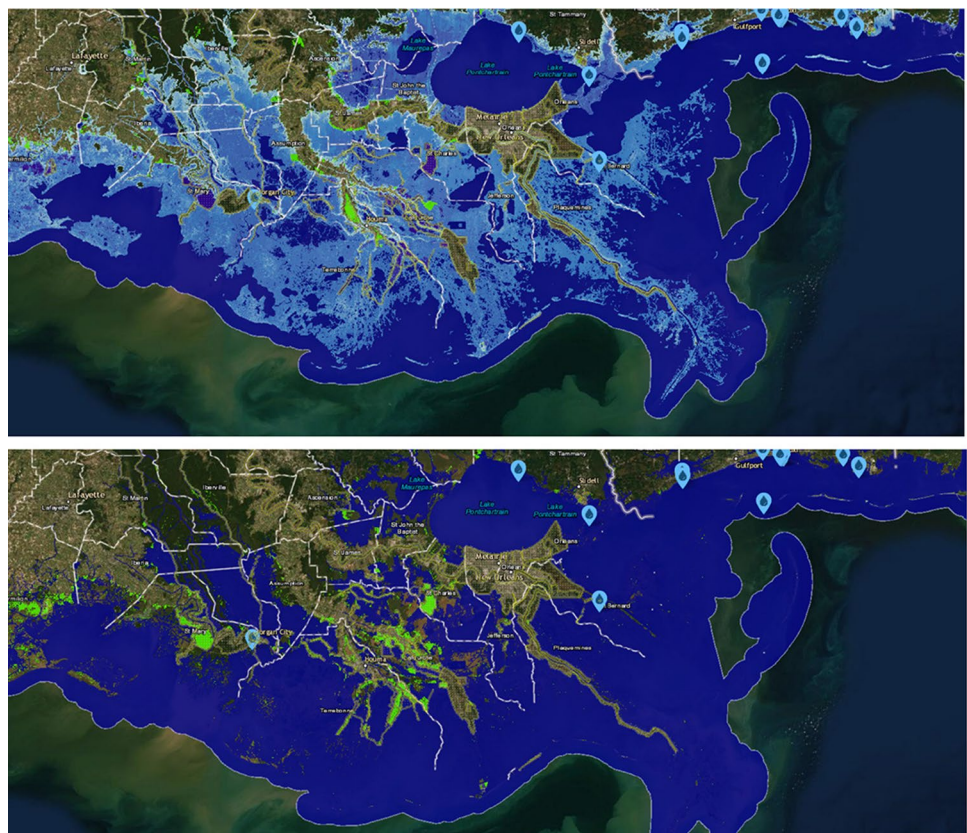
Fig. 4 Satellite view of the northern part of Venice lagoon, with indication of the various morphological features composing the lagoon environment. Note that in the Venice lagoon, sub-tidal flats and tidal flats are denoted as *bassifondi* and *velme*, respectively, while salt marshes are called *barene*

successful attempts have been made to classify and discuss the variety of definitions employed in the literature (Coco et al. 2013; Zhou et al. 2017). For these reasons, below we will not reexamine this aspect and refer the interested reader to the above contributions. We will limit ourselves to show that, based on our own research, the answer to the above question depends on various aspects. Below we analyze two of them. First, we show that the definition of *equilibrium* requires some care and different conclusions are reached depending on the actual definition employed. Second, we discuss how anthropogenic effects associated with social development have altered the *natural* trajectory followed by the evolution of many coastal lagoons. In addition, to illustrate the latter issue, we will refer to Venice lagoon, a very rich environment, containing most of the ingredients which affect the hydrodynamics and eco-morphodynamics of coastal wetlands. In addition, Venice lagoon is probably one of the most carefully monitored lagoon in the world and, due to the historical and cultural importance of Venice, ascertaining its fate in response to possible effects of global warming bears a great relevance.
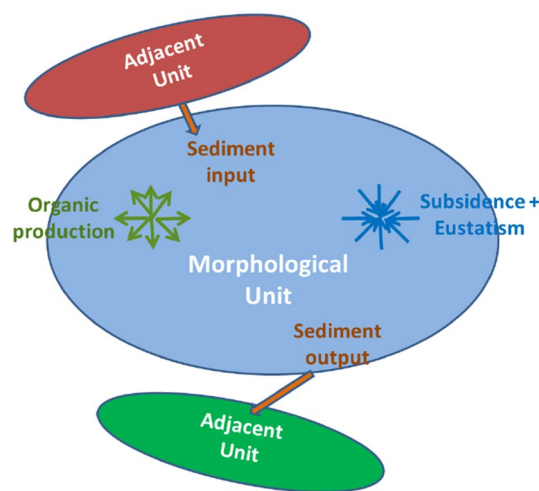
Fig. 5 Sketch of the sediment balance for each morphological unit of a lagoon

Our plan for the rest of the paper is to proceed as follows. First, (Sect. 2) we analyze distinctly the morphodynamic equilibrium of each of the morphological units composing a lagoon, namely channels (Sect. 2.1), inlets (Sect. 2.2), sub-tidal flats (Sect. 2.3) and intertidal features (intertidal flats—salt marshes) (Sect. 2.4). We then investigate how these distinct units interact and how this interaction modifies the transient response of the system to variations of the rate of sea level rise (Sect. 3). Next (Sect. 4), we discuss the variety of anthropogenic effects which may let the evolution of coastal lagoons deviate from their 'natural' trajectory. Finally (Sect. 5), we return to our original issue to draw some conclusions.

2 Equilibrium of distinct morphological units

Each morphological unit is an open system which exchanges mass (water and sediments) with its neighboring units. It may also contain a source of mass: indeed, marshes produce organic sediments resulting from the cyclic production, decomposition and compaction of biomass. In addition, in some sense, each morphological unit is also a sink for sediments which are effectively lost by the system as a result of two major natural processes, namely sea level rise and subsidence (Fig. 5). Hence, a simple general sediment balance equation for any morphological unit of a coastal lagoon may be written in the following form:

$$Q_{\text{in}} + Q_{\text{org}} = Q_{\text{out}} + A_u \sigma, \tag{1}$$

Here, Q_{in}, Q_{out} and Q_{org} are sediment fluxes averaged over a sufficiently long time. Q_{in} is the average flux of inorganic sediments supplied to the morphological unit by adjacent units; Q_{out} is the average flux of inorganic sediments lost by

the morphological unit to adjacent units; Q_{org} is the average flux of organic sediments produced within the unit. Moreover, A_u is the area of the morphological unit and σ is the spatially averaged rate of relative sea level rise due to both absolute sea level rise and subsidence.

The above simple statement immediately suggests an obvious observation: the long-term equilibrium of a morphological unit can hardly be considered independent of the morphological evolution of adjacent units. With this in mind, let us outline our present understanding of the morphodynamics of each unit.

2.1 Tidal channels

It proves convenient to start with *tidal channels*. Notable investigations of the morphodynamic evolution of these tidal features proceed from the works of Friedrichs (1995), Friedrichs and Aubrey (1996) and Schuttelaars and de Swart (1996), followed by Schuttelaars and de Swart (2000), Lanzoni and Seminara (2002), Tambroni et al. (2005), Todeschini et al. (2008), Tambroni and Seminara (2009), Seminara et al. (2010), D'Alpaos et al. (2010), Toffolon and Lanzoni (2010) among others (see also the review paper of de Swart and Zimmermann 2009).

Observations of the channel networks in Venice lagoon (Marani et al. 2002; Toffolon and Lanzoni 2010) suggest that lagoon channels are typically characterized by a funnel shape well approximated by an exponential law with aspect ratios falling in the range 15–35 and longitudinal bed profiles displaying an upward concavity. Proceeding landward, the grain size varies from fine sand close to inlets (mean grain size $d_{50} = 0.2 - 0.3$ mm) to very fine sand-silt (mean grain size $d_{50} = 0.05$ mm) (Magistrato alle Acque di Venezia 2008), with estimated critical bed shear stress τ_c^* of $0.15 - 0.16$ N/m², corresponding to a critical velocity U_c^* varying from 0.17 m/s at depths of the order of 1 m to 0.3 m/s at depths of the order of 10 m (in Sect. 2.1 and 2.2 a star superscript will denote dimensional quantities). Moreover, Friedrichs (1995) observed that the peak bottom stress at spring tide (as well as the associated peak of cross-sectionally averaged speed) keeps approximately constant along sheltered tidal channels at equilibrium. Hence, the net sediment flux also keeps constant.

The latter observations prompted a sequence of attempts to provide some theoretical understanding of the process. To present the latter developments in a unified framework, let us briefly introduce the general formulation of the problem. Following Seminara et al. (2010), let us then consider a straight tidal channel of length l^* with rectangular cross-section and width B^* varying exponentially landward (Fig. 6).
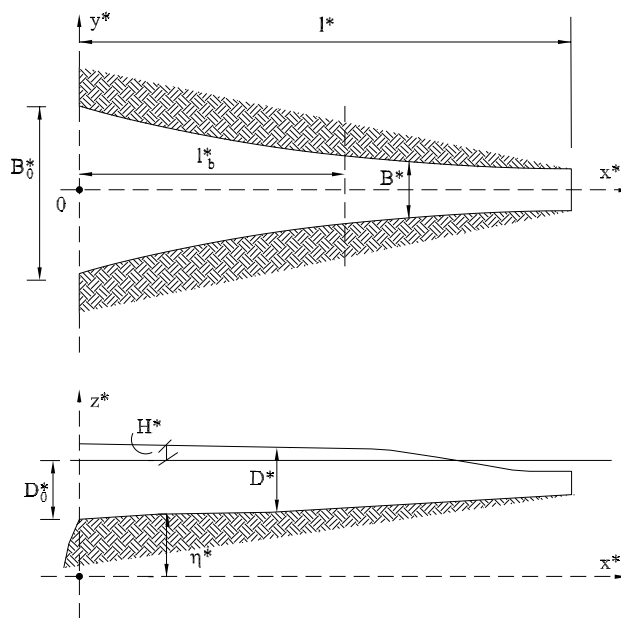
We then set

Fig. 6 Sketch of a tidal convergent channel and notations

$$B^* = B_0^* \exp(-x^*/l_b^*), \qquad (2)$$

where l_b^* is the convergence length, B_0^* is the inlet width and x^* is a longitudinal coordinate pointing landward with origin at the inlet.

In the context of a $1 - D$ model, the motion of the fluid phase is governed by the classical continuity and momentum (de Saint Venant) equations, which in dimensionless form, read

$$\lambda \frac{\partial D}{\partial t} + \epsilon \frac{\partial (UD)}{\partial x} - \epsilon \lambda_b (UD) = 0, \qquad (3a)$$

$$\lambda \frac{\partial U}{\partial t} + \epsilon U \frac{\partial U}{\partial x} + \frac{\partial H}{\partial x} + R \frac{U |U|}{c^2 D} = 0. \qquad (3b)$$

Here, independent and dependent variables have been scaled as follows:

$$\left(x, t, H, D, U, c\right) = \left(\frac{x^*}{l^*}, \omega^* t^*, \frac{H^*}{a_0^*}, \frac{D^*}{D_0^*}, \frac{U^*}{U_0^*}, \frac{C}{C_0}\right), \qquad (4)$$

where

- t^* denotes time and ω^* is the angular frequency of the forcing tide;
- D^* denotes the cross-sectionally averaged flow depth and D_0^* is the inlet depth at mean sea level;
- U^* denotes the cross-sectionally averaged flow speed and U_0^* is a characteristic flow speed set equal to the *inviscid* velocity scale $\epsilon \sqrt{g D_0^*}$, with g gravitational

222

Rendiconti Lincei. Scienze Fisiche e Naturali (2022) 33:217–243

acceleration and ϵ a dimensionless parameter measuring the relative tidal amplitude ($\epsilon = a_0^*/D_0^*$)
- H^* is the water surface elevation relative to the mean sea level and a_0^* is the amplitude of the forcing tide;
- C is the dimensionless Chèzy conductance (defined as the inverse of the square root of the friction coefficient) and C_0 is its value at the inlet reference conditions.

Further important dimensionless parameters appear in the governing equations: λ is the ratio between channel length and wavelength of a small amplitude inviscid tidal wave, R is a dimensionless parameter measuring the importance of friction relative to gravity in the momentum equation and λ_b weighs the relative effect of channel convergence in the continuity equation. They read

$$\lambda = \frac{l^* \omega^*}{\sqrt{g \, D_0^*}}, \qquad R = \frac{l^* \, \epsilon}{C_0^2 \, D_0^*}, \qquad \lambda_b = \frac{l^*}{l_b^*}. \tag{5}$$

Note that the above scaling is appropriate everywhere along the channel, except in the landward region where the bed emerges during part of the tidal cycle, hence the flow depth approaches zero. There, the flow depth scales with the tidal amplitude a_0^*: indeed, if details of the flow in this intertidal region are sought, the latter must be treated as a boundary layer where rescaling is necessary (Seminara et al. 2010).

The equations (3a) and (3b) must be supplemented by appropriate boundary conditions. At the channel mouth, we set

$$D|_{x=0} = 1 + \epsilon \, H(x,t)|_{x=0} = 1 + \epsilon f(t). \tag{6}$$

The landward boundary condition requires more care: in fact, the shoreline, located at $x_{sh}^*(t^*)$, is a moving boundary through which no relative flux may occur, hence,

$$U|_{x=x_{sh}} = \frac{\lambda}{\epsilon} \, \dot{x}_{sh}, \qquad D|_{x=x_{sh}} = 0, \tag{7}$$

where the dot denotes a time derivative. To close the mathematical formulation we need to couple hydrodynamics to morphodynamics through the $1 - D$ form of the evolution equation of the bed interface, expressing mass conservation of the solid phase (Exner 1925) which, in dimensionless form, reads

$$b \, T_0 \frac{\partial \eta}{\partial t} + \frac{\partial (b \, q_s)}{\partial x} = 0. \tag{8}$$

Here, b is the local channel width scaled by B_0^*, η is the local and instantaneous value of the laterally averaged bed elevation scaled by D_0^*, q_s is the total sediment flux per unit width scaled by $\sqrt{(\rho_s/\rho - 1) \, g \, d_{50}^3}$ (with d_{50} mean grain size, ρ_s sediment density and ρ water density) and T_0 is a dimensionless parameter which accounts for the fact that the time scale

of morphodynamics is typically much larger than the period of the forcing tide.

We can now define equilibrium more precisely: each property of the fluid and sediment motions must not exhibit net variations in a tidal cycle. This applies in particular to bed elevation. Let us then integrate (8) in a tidal period to find

$$\int_t^{t+2\pi} \frac{\partial (b \, q_s)}{\partial x} \, \mathrm{d}t = \frac{\partial \left(b \int_t^{t+2\pi} q_s \, \mathrm{d}t \right)}{\partial x} = 0. \tag{9}$$

It follows that, at equilibrium, the net sediment flux in a tidal cycle must be constant throughout the channel and the constant must vanish to satisfy the landward boundary condition imposed by the presence of a shoreline. Note that the above definition is consistent with the definition of dynamic equilibrium of type I proposed by Zhou et al. (2017).

Schuttelaars and de Swart (1996) considered short embayments ($\lambda \to 0$) with constant width ($\lambda_b \to 0$), neglecting friction and ignoring the landward boundary layer. Under these conditions, the equilibrium bed profile turned out to be a straight line and the flow was characterized by a spatially uniform bed shear stress. However, in the above work as in the later extension of Schuttelaars and de Swart (2000), the seaward boundary conditions employed over-constrained the problem, as the bed elevation at the sea entrance was fixed. This constraint was relaxed by Lanzoni and Seminara (2002) who solved the transient problem showing that, for given channel length, starting from an arbitrary initial bed profile, the flow and bed topography evolve in time and asymptotically tend to reach an equilibrium state characterized by vanishing net sediment flux in a tidal cycle. At equilibrium, a shore formed at the landward channel end and the bed elevation at the sea entrance reached some equilibrium value depending on channel length. This process was later reproduced in the laboratory by Tambroni et al. (2005) through long-term experiments which led to a very satisfactory agreement with numerical simulations of Lanzoni and Seminara (2002). Both experiments and numerical simulations showed that the effect of funneling was to induce a weak concavity of the bed profile. An important extension of the latter work was pursued by Todeschini et al. (2008) who showed that, if the initial length of the channel exceeds some threshold value, then the shore does no longer form at the landward end of the channel but inside the initial domain. Hence, provided the latter is sufficiently long, an equilibrium length of the channel is determined which depends only on channel convergence, tidal amplitude at the channel mouth and friction. Moreover, the stronger is the degree of convergence of the channel, the tidal amplitude at the mouth or the channel friction, the shorter is the equilibrium length. More recently, Seminara et al. (2010) performed a further step forward, including in the analysis the presence of tidal flats

flanking the main channel (treated as storage volumes) and the role of the intertidal wetting and drying region treated as an inner boundary layer with the help of a perturbation technique. A fully analytical solution was thus obtained, albeit under the constraint of *short* channel length. This solution, showed rigorously that, at least under the assumptions of the analysis, equilibrium was associated with a condition stronger than the vanishing of the net sediment flux in a tidal cycle. Rather, sediment transport at each instant of the tidal cycle had to vanish to achieve equilibrium. This solution was shown to agree quite well with the laboratory observations of Tambroni et al. (2005) (Fig. 7).

Moreover, tidal flats were shown to affect the channel hydrodynamics and cause shortening of the equilibrium length, the more so as the flats widen. The bed profile determined in the inner region agreed with the morphology of tidally dominated intertidal flats, which was determined by Friedrichs and Aubrey (1996) imposing that the tidal velocity should never exceed the threshold for sediment motion throughout the entire tidal cycle.

Finally, the above analytical solution was used by Tambroni and Seminara (2009) to provide a theoretical substantiation of the observation that sheltered tidal channels at equilibrium would satisfy an O'Brien–Jarrett–Marchi relationship between tidal prism P and average cross-sectional area Ω^* of the type established for tidal inlets (O'Brien 1969; Jarrett 1976; Marchi 1990), namely $P^* \approx \Omega^{*6/7}$. This suggestion has come from various Authors on the basis of field observations and numerical simulations (e.g., among others, Friedrichs 1995; Schuttelaars and de Swart 1996; Lanzoni and Seminara 2002; Van der Wegen et al. 2008; D'Alpaos et al. 2010).

Before we move to analyze the next morphological unit, the reader should be aware of the fact that the equilibrium configuration obtained so far satisfies Eq. (1) with vanishing values of Q_{in}, Q_{org}, Q_{out} and σ. If sediment supply does not vanish ($Q_{in} \neq 0$) then the channel eventually silts up or, alternatively, it may undergo a slow progradation-degradation of the equilibrium profile (Toffolon and Lanzoni 2010). Hence, in the absence of further sediment exchange with other neighboring units, equilibrium requires that the channel inlet adjusts to the constraint that the average net flux of sediments must vanish.

An interesting exercise performed by D'Alpaos et al. (2006) sheds some light on the effect of a persistent supply of sediments on the formation and evolution of the cross-section of a tidal channel consisting of an incision cutting through a flat-marsh platform which drains a given tidal watershed. This simplified model ignored longitudinal variations of the flow field and of the channel morphodynamics. Channel evolution arose from deposition on the marsh platform and erosion-deposition in the channel, mediated through their effect on the tidal prism flowing through the cross-section. The analysis suggests that, as the marsh platform emerges, the consequent reduction of the hydro-period leads to channel infilling. D'Alpaos et al. (2010) conclude that an equilibrium condition can only be maintained provided the rate of sea level rise attains some given value.

2.2 Lagoon inlets

Due to its conceptual and practical implications, the equilibrium of tidal inlets has been widely investigated since O'Brien (1931) proposed a linear relationship between the inlet cross-sectional area (below mean sea level) and the tidal prism, based on observations on inlets located on the Pacific coast of the United States. The linear relationship was later corrected by the same author (O'Brien 1969), using data collected on a large number of tidal inlets located in North America. The well-known relationship between the minimum cross-sectional area Ω^* of the inlet channel at mean sea level and the tidal prism P^* was then proposed:

$$\Omega^* = K P^{*m}, \tag{10}$$

with $K = 2.43 \times 10^{-4}$, $m = 0.85$ and the quantities Ω^* and P^* expressed in m^2 and m^3, respectively. The validity of a power law relationship was confirmed by subsequent studies (Jarrett 1976; Bruun 1978; Hughes 2002), with m typically lying in the range 0.85–1.10. In particular, Jarrett (1976) determined K and m distinguishing among various groups of inlets located along the North American coast, depending

Fig. 7 Comparison between the equilibrium bed profile predicted by Seminara et al. (2010) and that observed after 2000 tidal cycles by Tambroni et al. (2005) for a constant width channel, using either a constant or a spatially variable Chézy coefficient

224

Rendiconti Lincei. Scienze Fisiche e Naturali (2022) 33:217–243
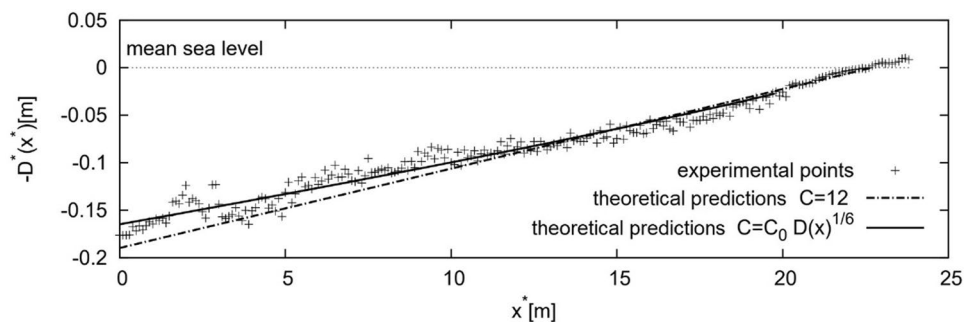
on their location (Atlantic, Pacific, or Gulf of Mexico) and the number of jetties they contained. Note that the variability of K and m embodies further effects, e.g., the intensity of littoral drift, the size of sediments, the hydraulic resistance of the inlet, not accounted explicitly in (10).

Various authors (e.g., Escoffier 1940; Krishnamurthy 1977; Marchi 1990; Hughes 2002; D'Alpaos et al. 2009) have attempted to provide some theoretical substantiation of the relationship (10). All these approaches relied on the assumption that, at equilibrium, the maximum bottom shear stress should attain the threshold value for sediment motion. In particular, Marchi (1990) was able to prove that, with the above assumption, the exponent m takes the exact value $6/7 = 0.857$.

More recently, Tambroni and Seminara (2009) revisited the problem following an approach similar to that presented for tidal channels (Sect. 2.1). They considered a straight tidal channel of length l^*, rectangular cross-section and constant width B^* connecting the open sea with a closed basin with surface area S^* (Fig. 8).

The mathematical formulation of the hydrodynamic problem does not differ from that presented in Sect. 2.1 (with $\lambda_b = 0$) except for the boundary condition at the inner boundary ($x = 1$). Here we may impose flow continuity requiring that the flow discharge through the landward cross-section of the inlet channel must balance the rate at which volume is accumulated into (or subtracted from) the basin. This condition is readily implemented if a *static* model for the basin hydrodynamics is employed, assuming that the free surface keeps horizontal throughout the basin, an assumption valid when the size of the latter is much smaller than the length of the tidal wave. In dimensionless form, one finds

$$\gamma \left[UD \right]_{x=1} = \left. \frac{\mathrm{d}H}{\mathrm{d}t} \right|_{x=1}, \qquad \gamma = \frac{B^* \sqrt{g D_0^*}}{\omega^* S^*}. \tag{11}$$

With the latter condition, the mathematical problem is readily solved (Tambroni and Seminara 2009). At the leading order of approximation, one finds
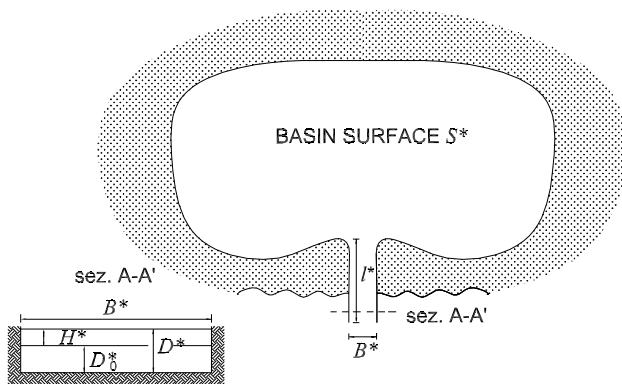

Fig. 8 Sketch of a tidal inlet and notations

$$H = f(t), \qquad U = \frac{\dot{f}}{\gamma D(x)}. \tag{12}$$

Let us now examine the issue of equilibrium. The constraint to be satisfied is that the net sediment flux in a tidal cycle must be constant throughout the channel as prescribed by Eq. (9). This requirement is weaker than the assumption made by the various authors who attempted to provide a theoretical substantiation of (10), namely that the flux must vanish identically at any cross-section. Given the form (12) of the solution for U, the latter condition requires that $D^*(x)$ keeps constant ($= D_{eq}^*$) and U^* be a function of time such that $max \, |U^*| = U_{cr}^*$, with U_{cr}^* threshold value of the flow velocity for the inception of sediment motion. Employing the Strickler relationship for the Chézy flow conductance, Tambroni and Seminara (2009) then derived the following relationship for the inlet flow depth at equilibrium:

$$D_{eq}^* = \left(\frac{S^* \omega^* a_0^*}{B^* k_s^*} \frac{|\dot{f}|_{max}}{\sqrt{\theta_{cr}(\rho_s/\rho - 1) d_{50}}} \right)^{6/7}, \tag{13}$$

with k_s^* Strickler's coefficient, θ_{cr} critical value of the Shields parameter (i.e., of the dimensionless bed shear stress) and a_0^* amplitude of the forcing tide. Moreover, the above solution leads to a relationship between the tidal prism and the inlet cross-sectional area at equilibrium, identical with Eq. (10) with $m = 6/7$. However, when applied to the inlets of Venice lagoon, Eq. (13) suggests that inlet equilibrium would require flow depths much larger than those observed. In addition, indeed, to fit Venice data, Marchi (1990) was forced to assume values of the dimensional critical bed shear stress as large as 4 N/m², much larger than the values characteristic of fine sand (for $d_{50} = 0.2$ mm, $\tau_c^* = 0.17$ N/m²). This is not surprising if one recognizes that if inlet equilibrium were associated with the threshold conditions for sediment motion then the net sediment flux exchanged by the inlet with the sea should vanish. However, this is not the case, at least in general. In a tidal inlet, the sediment flux imported from the sea during the flood phase is not controlled by the transport capacity of the flood currents, but rather by the capacity of sea waves to resuspend sediments in the surf zone. Resuspension overloads the flood currents which then deposit their load inside the inlet. Indeed, a sand particle of size 0.2 mm settles over a depth of 10 m in a time of the order of 500 s, hence at a distance of the order of 500 m from the entrance. On the contrary, the sediment flux exported to the sea during the ebb phase is controlled by the transport capacity of the ebb stream which would vanish at equilibrium. Hence, for an inlet to be in equilibrium, its depth must adjust such that the sediment transport capacity of the inlet stream allows it to export the average flux of sediments imported by the sea during storm events.

2.3 Sub-tidal and tidal flats

Let us next consider sub-tidal and tidal flats, shallow, fairly flat or weakly sloping features typically cut through by tidal channels and bounded by marshes (e.g., Fig. 4). In Venice lagoon sub-tidal flats lie approximately in a range between 0.6 and 2.0 m below m.s.l., while tidal flats lie in the range 0.6–0 m below m.s.l.. Their evolution is controlled by the sediment balance (1) where, with reference to the transect of Fig. 9, Q_{in} is the average net flux of sediments supplied by the channel in the flood phase, Q_{org} vanishes and Q_{out} is the sum of the average net flux of sediments lost to the channel in the ebb phase plus the average net flux of sediments lost to the marsh in the flood phase. Note, that marshes effectively act as sinks for sediments.

The simplest model one may envisage to describe the morphodynamic evolution of a tidal flat is a *zero-order model*, namely a model which ignores the spatial structure of the flat and simulates the rates of accretion and submergence processes only along the vertical direction. These models stem from the pioneering works of Randerson (1979) and Krone (1987) developed to investigate the morphodynamic evolution of salt marshes. The only conservation equation they employ is a spatially averaged balance of sediment mass which, in dimensional form, reads (Fig. 9)

$$\frac{d\bar{\eta}}{dt} = a_{min} - s_{sub} - s_{slr} - s_{res}. \tag{14}$$

Here, $\bar{\eta}$ is the spatially averaged elevation of the tidal flat, a_{min} is the average net accretion rate driven by inorganic (minerogenic) sediments supplied by the channel adjacent to the flat and settling on the flat platform during the flood phase, s_{sub} is the rate of increase of flat submergence arising from regional soil subsidence, s_{slr} is the rate of increase of flat submergence arising from regional sea level rise and s_{res} is the rate of increase of flat submergence driven by wind wave sediment resuspension leading to a loss of sediment towards the channel (during the ebb) or the salt marsh (during the flood). Note that, in Eq. (14), it is implicitly assumed that tidal currents alone are unable to entrain sediments, i.e., entrainment is only driven by the stresses that wind waves generate on the bottom.

The sediment conservation Eq. (14) immediately suggests a puzzling question: flat equilibrium ($d\bar{\eta}/dt \equiv 0$) requires that the concentration of suspended sediment in the adjacent channel be sufficiently high, such that the sediment flux supplied by the flood currents to the tidal flat balances the tendency of the latter to increase its submergence due to subsidence, sea level rise and sediment resuspension by wind waves. Hence, for a flat to be in equilibrium, the adjacent channel cannot be also in equilibrium, at least not in the condition of static equilibrium that we discussed in Sect. 2.1. But, is a dynamic channel equilibrium possible? We delay an answer to this question to Sect. 3.

To make progress with the balance Eq. (14), once the regional values of subsidence and sea level rise are known, one needs to quantify a_{min} and s_{res}. Estimating the latter two quantities in the context of a $0-D$ model is quite hard. Marani et al. (2007) write

Fig. 9 Sketch of a tidal flat with indication of the various contributions to the sediment balance. *m.s.l.* mean sea level, *m.h.t.* mean elevation of high tides, *m.l.t* mean elevation of low tides
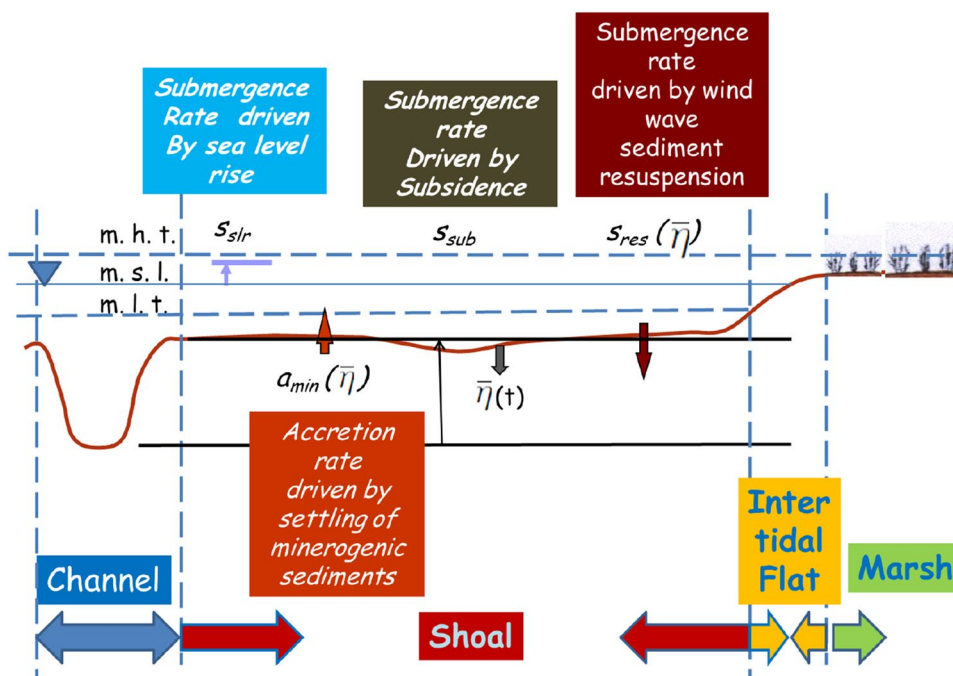
$$a_{\min} = \frac{1}{T} \int_0^T \frac{C(t, \bar{\eta})\, W_s}{\varrho_s}\, dt, \tag{15}$$

with $C(t, \bar{\eta})$ local and instantaneous value of the depth averaged sediment volumetric concentration, depending on the mean elevation of the tidal flat, W_s settling speed of sediment particles and ϱ_s particle density. Note that the value of the concentration that should appear in (15), namely the concentration at the flat platform, has been approximated by the depth-averaged concentration. The function C depends on the history of past resuspension events, sediment supply from the channel and sediment loss to the marsh. Its knowledge would require the solution of a full advection diffusion equation, coupled to the knowledge of external inputs and of the effects of wind resuspension. However, in the context of $0 - D$ models this is obviously impossible and some unavoidably severe approximation is needed. Marani et al. (2007) derive the function $C(t, \bar{\eta})$ solving an ordinary differential equation that, in the absence of sediment trapping due to macroalgae and/or aquatic fanerogams, reads

$$\frac{d\big[h(t) - \bar{\eta}\big]\, C(t, \bar{\eta})}{dt} = -W_s\, C(t, \bar{\eta}) + \tilde{C}_0\, \frac{dh}{dt} \tag{16}$$

Here, we denote by $h(t)$ the free surface elevation (approximated as horizontal) and by $\tilde{C}_0$ the depth-averaged concentration at the inlet cross-section of the flat. The latter quantity is assumed to take different values in the flood and ebb phases. More precisely, flood currents are assumed to carry a fixed concentration C_0, representing external sediment availability, while the concentration of outgoing ebb currents is the instantaneous depth averaged concentration $C(t, \bar{\eta})$. Note that the above authors did not include wind resuspension effects in (16), thus assuming that all the entrained sediments are lost to the neighboring environments and no sediment resettles in the flat.

Finally, the quantity s_{res} was assumed to be proportional to the tidally averaged value of the excess bottom stress relative to its threshold value for bottom erosion. The bottom stress was evaluated as proportional to the square of the amplitude of the wave flow speed at the bottom and the latter quantity was associated to the wind speed assuming fully developed conditions for the wave (no influence of fetch) and adopting the linear approximation. The critical stress was given two different values depending on the depth of the flat platform and the consequent presence or absence of stabilizing polymeric bio-films produced by benthic microbes.

The output of the above analysis is plotted in Fig. 10 where R denotes the relative rate of sea level rise ($R = s_{\mathrm{sub}} + s_{\mathrm{slr}}$). The authors consider a 20th-century scenario appropriate to Venice lagoon, characterized by a rate of sea-level rise of 2 mm/year and a local subsidence of 1.5 mm/year, for a total $R = 3.5$ mm/year. Moreover, they
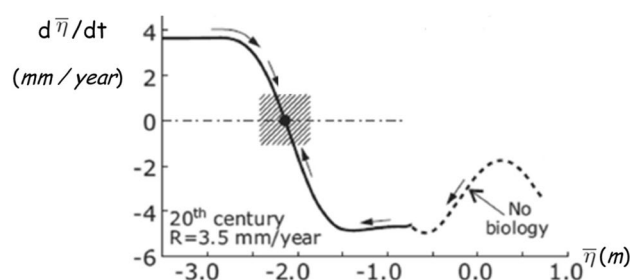
Fig. 10 Trajectory of the morphodynamic evolution leading to a stable state of the flat, under a scenario of 3.5 mm/year relative sea level rise and assuming that no biological activity is present (modified from Marani et al. 2007)

considered a micro-tidal environment ($a_0^* = 0.74$ m) and assumed $C_0 = 20$ g/m³, $d_{50} = 50$ μm and $W_s = 0.2$ mm/s. Figure 10 shows that, under these conditions and in the absence of any biological control, the only equilibrium state is sub-tidal and it is stable. Stability arises from a simple feedback mechanism: the stress induced by wind waves tends to vanish as the flow depth tends to infinity. Hence: a small positive perturbation of the flat depth in a neighborhood of sub-tidal equilibrium leads to a reduction of sediment resuspension by wind waves. Consequently, the erosive effect of wind waves no longer balances the accretion rate of the flat platform induced by settling: in other words, this feedback mechanism tends to reestablish the previous state. A tidal flat equilibrium does not exists for the above conditions and is found to be possible only within a narrow range of the rate of relative sea level rise ($0 < R < 1.8$ mm/year). The equilibrium is stable within a fairly narrow range of values of the platform elevation ($0.27 < \bar{\eta} < 0.74$ m a.m.s.l). The ranges of R and $\bar{\eta}$ for which a stable tidal flat equilibrium state can exist widen ($3.9 < R < 7.2$ mm/year and $-0.74 < \bar{\eta} < 0.74$ m a.m.s.l, respectively) when accounting for the stabilizing action associated with the presence of a polymeric bio-film produced by microphytobenthos. In any case, for $R > 7.2$ mm/year also the sub-tidal equilibrium disappears and the flat platform deepens indefinitely.

The above results are of conceptual interest as they suggest the possibility that a condition of dynamic morphodynamic equilibrium might indeed be reached. The latter depends crucially on the availability of sediments in the channels adjacent to the flat parameterized by the input concentration C_0. Field observations (e.g. Mariotti and Fagherazzi 2012) do support the existence of a basically asymmetric exchange of sediments between the channel and the flat whereby flat receives sediments from the channel during the flood and looses sediments to the channel in the ebb, a process that the latter authors called *spillover mechanism*. However, as mentioned above, this raises the problem of how the channel equilibrium can be maintained.

At last, note that a zero-order model, besides its intrinsic limits, has a major drawback: it assumes that the horizontal domain keeps unchanged throughout the evolution process. This is not the case in general: the boundary between marshes and flats evolves depending on the morphodynamic evolution of the two environments. This is a major issue which will deserve attention (Sect. 3). But before we tackle the latter problem, let us briefly review the available knowledge on the morphodynamics of salt marshes.

2.4 Marshes

Salt marshes are intertidal features: in Venice Lagoon they lie at an average elevation between 0.1 and 0.5 m above m.s.l.. Their distinct feature is the presence of halophytic vegetation (e.g., Cronk and Fennessy 2001), which plays a major role in marsh evolution. Salt marshes are sites of great biodiversity and, as such, the major as yet unresolved issue of whether coastal wetlands will submerge in response to an acceleration of sea level rise has attracted a great attention from the scientific community.

Like for flats, most of the modeling efforts until recently have concentrated on zero-order models, which are thoroughly reviewed by Kirwan et al. (2010) and Fagherazzi et al. (2012). Here, we simply recall their main achievements. The common characteristics of these models are: (1) marsh evolution is decoupled from the coevolution of the adjacent morphological unit (flats) modeled as steady sources of minerogenic sediments; (2) marsh properties are spatially averaged. The novel feature to be included when formulating the mass conservation equation for the marsh is then the role of vegetation. On one hand, vegetation affects the marsh hydrodynamics. Increasing friction and damping turbulence (Nepf 1999; Leonard and Luther 1995; Leonard and Croft 2006; Neumeier 2007), it opposes sediment resuspension and enhances inorganic sedimentation (Gleason et al. 1979; Morris et al. 2002), which is driven by natural settling of suspended particles and by the capture of particles on plant stems (Yang et al. 2008). As a result, marshes play the role of sinks for suspended sediments (e.g., Christiansen et al. 2000; Mudd et al. 2004; Le Hir et al. 2007). Vegetation also produces organic sediments through the growth, death and decomposition of above-ground and below-ground biomass, a process strongly dependent on the flow depth and, hence, on the inundation period (hydroperiod) characterizing the marsh platform (Morris et al. 2002; Mudd et al. 2009). This additional feature gives rise to further feedback effects: sediment supply to the marsh, as well as sea level rise and subsidence, affect the flow depth on the marsh, modifying the production of biomass which in turn influences marsh accretion. Note that, as pointed out by Fagherazzi et al. (2012), below-ground production may be

quite an important process under certain conditions, such to account for a relatively large fraction of marsh accretion (Callaway et al. 1997; Nyman et al. 2006), and reaching values of annual organic matter accumulation rate as high as 1.7 kg/m^2 (Chmura et al. 2003). Finally, organic sediments undergo compaction, i.e., a progressive reduction of their void ratio under the action of the upper load which acts as an effective stress (Gutierrez and Wangen 2005).

Accounting for all the above processes, the continuity equation (14) has to be modified for marshes as follows (Krone 1987):

$$\frac{\mathrm{d}\bar{\eta}}{\mathrm{d}t} = a_{\min} + a_{\mathrm{org}} - s_{\mathrm{com}} - s_{\mathrm{slr}} - s_{sub}, \qquad (17)$$

where $\bar{\eta}$, $a_{\min}$, s_{slr} and s_{sub} have the same meaning as in Eq. (14), a_{org} is the accretion rate induced by the production of organic sediments on the marsh and s_{com} is the rate of increase of marsh submergence arising from compaction of sediment deposits (Fig. 11). Note that both $a_{\min}$ and a_{org} are functions of the biomass density B, namely the mass of vegetation present on the marsh per unit surface.

A number of zero-dimensional models have been proposed in the literature. The early models, where the feedback of flow depth variations on the production of organic sediments was absent (Randerson 1979; Krone 1987; Allen 1990; French 1993) reached the conclusion that the marsh platform would always keep pace with relative sea level rise as, increasing the latter, the sedimentation rate would also increase. Drowning of the marsh would only arise under the most severe assumptions on the relative sea level rise (French 1993).

The important investigation of Morris et al. (2002) modified the latter picture. Based on detailed and systematic field observations, the latter Authors were able to clarify the dependence of biomass productivity on marsh elevation relative to mean sea level (Fig. 12). More precisely, they showed that both upper and lower limits of marsh elevation for the productivity of *Spartina Alterniflora* exist and pointed out that the dependence of productivity on the flow depth D "......*satisfies the ecological principle that a plant's distribution will span a range of tolerance to an abiotic variable, like flooding depth, with an optimum somewhere in the middle of the range......*".

To determine possible equilibrium states, Morris et al. (2002) imposed that the net accretion rate of the marsh platform, driven by minerogenic and organic production and assumed to be proportional to both flow depth and biomass productivity, should equal the relative sea level rise. Feeding the observed dependence of biomass productivity on flow depth into the equilibrium statement, the authors were able to show that, in accordance with the observations of Allen (1995), marshes situated at less

Fig. 11 Sketch of a marsh with indication of the various contributions to the spatially averaged sediment conservation equation
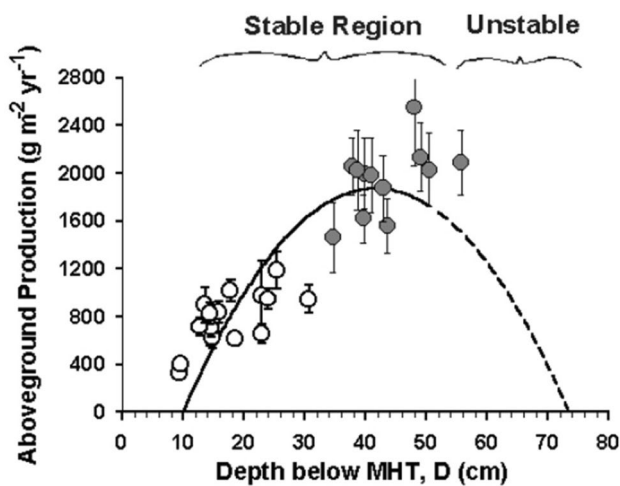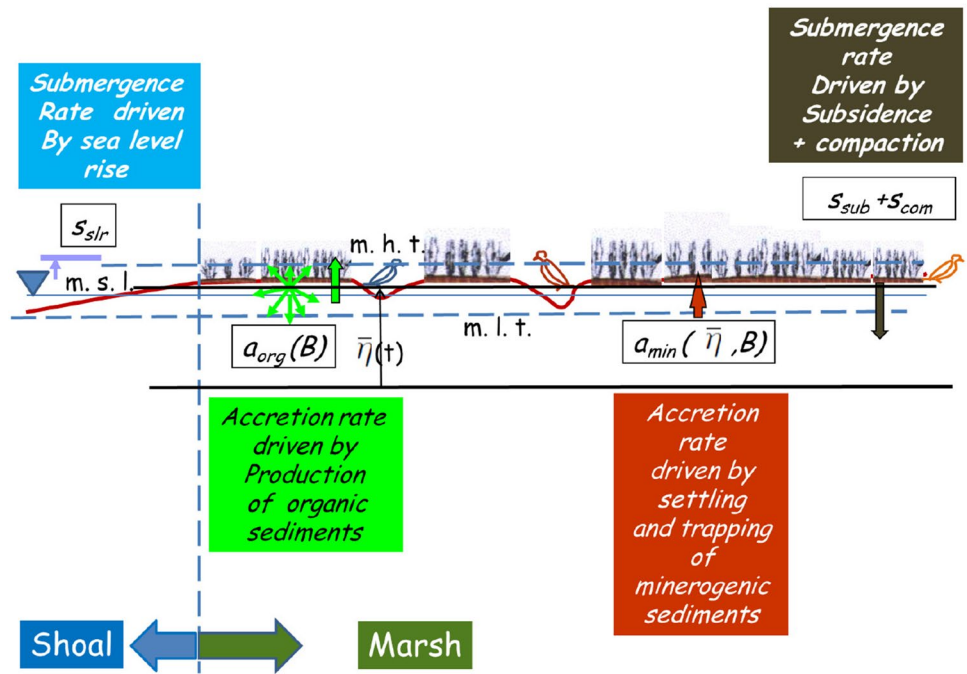
Fig. 12 Relationship between the measured productivity of the salt marsh macrophyte S. Alterniflora and the depth below mean high tide (MHT) of sites in the high (o) and low marsh (•). The experimental points (o) denote stable states, the points (•) denote unstable states (reproduced from Morris et al. 2002)

than optimum depths are stable against perturbations of mean sea level. On the contrary, sub-optimal marsh elevations are unstable. More recently, Mudd et al. (2009) improved upon the previous model developing a quantitative description of the life-cycle of biomass, including its growth and mortality both below- and above-ground.

A somewhat different description of biomass evolution, based on the logistic model (Levins 1969), was employed by Marani et al. (2007). The logistic equation appears to

be a more powerful and general approach, which is able to describe both the behavior of *Spartina Alterniflora* which exhibits a maximum productivity at an optimal depth and the behavior of Mediterranean and northern European marshes, where, according to Silvestri et al. (2005), due to the competition among numerous halophytic species, biomass is a monotonically increasing function of elevation. The approach of Marani et al. (2007) was able to detect two distinct equilibria. The former, associated with tidal flats, is characterized by the absence of vegetation and has been discussed in Sect. 2.3.

The latter, including the effect of vegetation, is associated with marshes. With the data presented in Sect. 2.3, the second equilibrium appears for $2 < R < 3.9$ mm/year and values of R larger than 3.9 mm/year lead to a transition from a marsh to a tidal flat equilibrium (Fig. 13).

A different scenario meant to model typical pre-sixteenth century conditions of Venice lagoon was also analyzed assuming a basal concentration ($C_0 = 40$ g/m^3) twice as large as the one taken to be characteristic of the twentieth century. The model predicted that at that time "*.....deposition dominated over erosion and the lagoon tended toward a configuration dominated by high marshes, in which tidal flats and sub-tidal platforms were disappearing.....*". Saying this in other terms: the 'natural' lagoon was very far from being in equilibrium.

A number of works of the same group of researchers (Fagherazzi et al. 2006, 2007; Defina et al. 2007; Marani et al. 2010) have further developed the previous approach. Essentially, Fagherazzi et al. (2006) show that "*...the bimodal distribution of equilibrium elevations stems from*
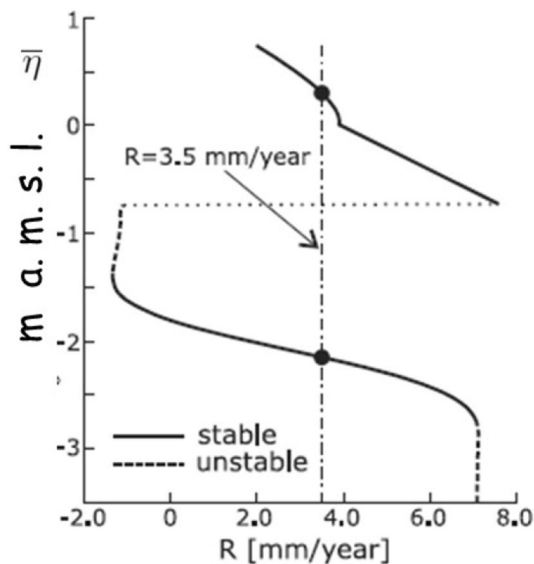
Fig. 13 Dynamics of a Venice-like tidal system in the twentieth-century scenario according to Marani et al. (2007): the bifurcation plot shows the ranges of R for which stable states (solid lines) and/or unstable states (dotted lines) exist. The dash-dot line indicates the best-estimate $R = 3.5$ mm/year for the Venice lagoon in the twentieth century (modified from Marani et al. 2007)

the characteristics of wave induced sediment resuspension, and, in particular, from the reduction of maximum wave height caused by dissipative processes in shallow waters....." and "...*areas at intermediate elevations are inherently unstable and tend to become either tidal flats or salt marshes....*". These conclusions were later confirmed through numerical models (Fagherazzi et al. 2007; Defina et al. 2007) where the effect of tidal currents, ignored in zero-dimensional models, was included and proved to affect the equilibrium of tidal flats significantly. The important conclusion of Marani et al. (2010) was that "*.... marshes and tidal flats are not equilibrium landforms....*".

Let us finally come to the major issue concerning the response of marshes to variations of the rate of sea level rise. Field observations do indeed suggest that, for many marshes, accretion rates have been tightly connected with the rate of sea level rise (Cahoon et al. 1997; Friedrichs and Perry 2001; French 2006). In addition, examples are known of wetlands which have been able to adjust to relatively slow sea level rise for a few thousands years (Redfield 1965). However, in the last two–three centuries the rate of sea level rise has shown some acceleration: from a fairly constant value, ranging around 1 mm/year to 2–3 mm/year (Church and White 2006; Jevrejeva et al. 2008; Gehrels et al. 2008). In addition, a number of field observations show that coastal wetlands are deepening or disappearing in various regions of the world (e.g., Stevenson et al. 1986; Reed 1995; Swenson and Swarzenski 1995; Day et al. 1999; Kearney et al. 2002;

van der Wal and Pye 2004). Ascertaining to what extent this has to be attributed to the limited ability of marshes to adapt to the new regime of sea level rise is not easy as the latter effect cannot be isolated from the number of further anthropogenic effects which may have contributed to perturbing the state of the system (Sect. 4). This notwithstanding the exercise of investigating the threshold conditions for platform submergence as predicted by zero-order models proves of some interest. Kirwan et al. (2010) performed this exercise comparing results of five different numerical models which included different dominant mechanisms. Results were strongly dependent on tidal range and sediment supply, low values of the latter quantities being associated with low thresholds for the rate of sea level rise and vice versa. Under conditions of high sediment availability marshes are predicted to be strongly resilient to sea level rise, being able to survive rates as high as several cm/year (Fig. 14).

3 Morphological interactions

Results discussed in the previous section, besides ignoring horizontal variations of the system, also ignore the morphological interactions between adjacent environments. Accounting for the latter effect modifies the picture significantly.

Tambroni and Seminara (2012) investigated the latter problem considering a model system including most ingredients which control the morphodynamics of a lagoon system. The model was, however, sufficiently simple to allow long-term numerical simulations. It consisted of a $1 - D$ configuration including a tidal channel merging into a $1 - D$ flat bounded by a $1 - D$ marsh. Starting from some initial configuration of the channel these authors modeled how a flat-salt marsh system forms at the landward end and determined the long-term evolution of the system under different scenarios of relative sea level rise.

Tide propagation in the channel domain was modeled following the $1 - D$ approach of Lanzoni and Seminara (2002). At the channel inlet sea level fluctuations were prescribed, while, at the landward domain end, the boundary condition changed throughout the simulation. In the initial phase (bed permanently submerged) the normal component of the velocity at the land boundary was simply set to vanish. As the deposition process led to emergence of the bed and salt marsh formation, the wet and dry region where the shoreline oscillates back and forth was modeled following the approach of Defina (2000). The effect of wind, blowing either in the seaward or landward direction, was accounted for assuming some random succession of wind events with assigned frequency distribution for the wind speed. Wind generated waves were also modeled. Their amplitude in shallow waters is spatially dependent and is mainly controlled
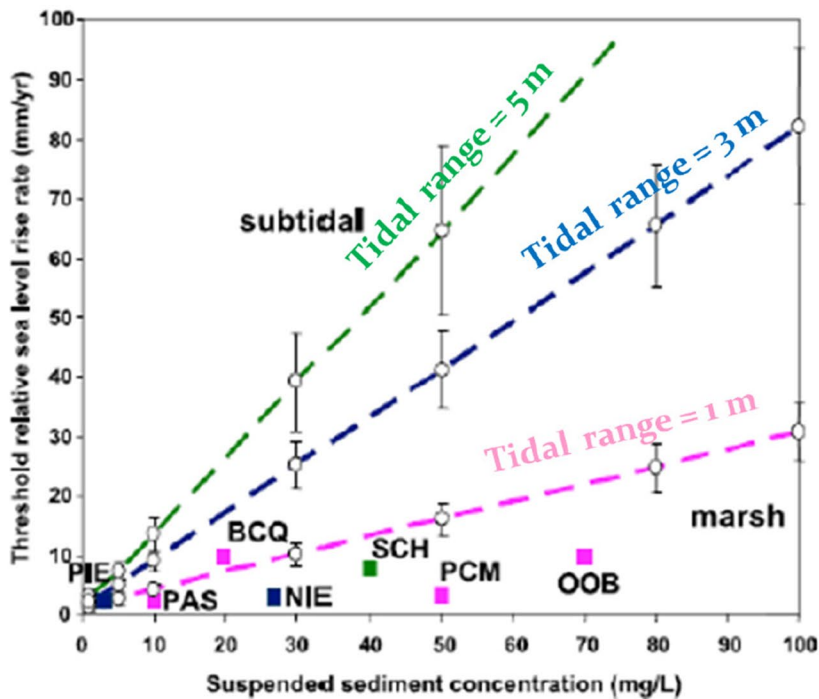
Fig. 14 Results obtained by Kirwan et al. (2010), comparing threshold rates of sea level rise for marsh submergence obtained by five different numerical models, as a function of rate of sea level rise for three different values of the tidal range. Squares refer to selected marshes with different characteristics (reproduced from Kirwan et al. 2010)

by shoal depth, wind intensity and available fetch. Their development also depend on energy spreading through non linear interactions, frictional dissipation, wave breaking and the presence of obstacles, such as islands. The wave field was modeled using the empirical relationships derived by Young and Verhagen (1996) from field observations performed in shallow environments. The sediment flux under the combined actions of wind waves and tidal currents was evaluated employing the approach proposed by Fredsoe and Deigaard (1992). A second independent contribution to the sediment flux due to the effect of the currents driven by wind stress and wind setup was also accounted for. Finally, at the channel inlet, two distinct boundary conditions were tested: either assuming that sediment transport was determined by the local transport capacity of the stream at both flood and ebb, or imposing a given sediment concentration at flood to investigate the effects of a possible excess or deficit of sediment supply. At the land boundary, the exchange of sediments between the channel and the marsh was modeled assuming different conditions throughout the tidal cycle. In the flood phase, the sediment flux entering the marsh was determined by the transport capacity of the stream at the last channel section. On the other hand, during the ebb phase, the sediment flux leaving the marsh was determined by the residual sediment available to the tidal current after settling and trapping by vegetation.

In the marsh domain, the model of tide propagation was modified such to account for the frictional effects of vegetation which depend on the spatial density of biomass associated with above-ground halophytic vegetation (Nepf 1999). Prediction of the growth and decay of both above- and below-ground vegetation was based on the model by Mudd et al. (2009) which explicitly accounts for both the labile and refractory fractions of biomass. The presence of vegetation over the marsh prevents the occurrence of bed load transport as well as of sediment resuspension (Mudd et al. 2010). Hence, to estimate the rate of marsh accretion a_{min} driven by deposition of minerogenic sediments, Tambroni and Seminara (2012) solved a pure settling-advection equation for the mean concentration C averaged over turbulence, neglecting turbulent diffusion as the presence of vegetation has a strong damping effect on the turbulence of the stream. Results of the investigation can be summarized as follows.

3.1 Evolution of the channel-flat system in the absence of vegetation

We have already discussed in Sect. 2.1 the simplest configuration analyzed by Lanzoni and Seminara (2002) and Seminara et al. (2010). Provided sediment supply at the inlet equals transport capacity and in the absence of both wind and sea level rise, the channel eventually reaches a static

equilibrium with a shore at the inner end of the channel and the sediment flux vanishing everywhere (Fig. 7). On the contrary, no equilibrium is possible if a non-vanishing sediment flux is supplied at the inlet. A non-vanishing rate of relative sea level rise R reestablishes the possibility of equilibrium which, however, would require that $\langle q_s \rangle_{x=0} = R\,l$, with l the domain length excluding the marsh portion and $\langle q_s \rangle$ the net tidally averaged sediment flux per unit width. Nevertheless, the net tidally averaged sediment flux at the inlet is a quantity which is not controlled by sea level rise hence, again, exact equilibrium can hardly be established and the channel will slowly either degrade or fill up.

Illustrating the effects of wind requires some care. As mentioned above, wind exhibits two main effects: (1) it generates waves which resuspend sediments through the wave driven stress in the bottom boundary layer and possibly through the turbulence generated by wave breaking; (2) it generates a stress at the surface and consequently a wind set up which drives a return flow which advects sediments in the direction opposite to the wind direction. Let us then consider a wind blowing in the seaward direction but neglect the effect of wind setup. Recall that, using the linear wave theory, the maximum shear stress generated by the wave τ_w is proportional to the square of the significant wave height and inversely proportional to the square of $\sinh(kD)$ with D flow depth and k wavenumber. In the shoaling region of the channel, close to the marsh boundary, the water depth increases seaward and the wave develops as the fetch increases. Hence, proceeding from the marsh seaward, the wave bottom stress initially increases, reaches a peak at some distance from the marsh border and then gradually decreases. A similar trend is exhibited by sediment transport which increases landward up to a peak and then decreases (Fig. 15a). As a result, in the region of the shoal located between the border of the unvegetated platform and the area close to the stress peak sediment deposits while erosion occurs when proceeding further seaward. Hence, the platform progrades and its border steepens, while the channel continuous to erode. No equilibrium was found after a 1000-year simulation (Fig. 15b). Note that, in a work which tackles essentially the same problem with partly different approaches, Mariotti and Fagherazzi (2010) claim to find equilibrium with a non vanishing sediment concentration prescribed at the inlet. It is hard to interpret this finding in the light of the results discussed above.

The above $1 - D$ models of an unvegetated channel-flat system assume that the along channel distribution of the cross-section width is prescribed a priori. This restriction was relaxed by Lanzoni and D'Alpaos (2015), who investigated the three-dimensional equilibrium of a rectangular basin formed by a channel flanked by an intertidal platform. The degree of channel funneling was not imposed a priori, but was determined numerically computing the shape and size of channel cross-sections at equilibrium. The tidal

system was assumed to be short enough that, at any instant of the tidal cycle, the water surface elevation could be taken as horizontal and, hence, the tide propagated quasi-statically. The water surface discharge at a given transect was then computed straightforwardly as the rate of change of the volume of water lying upstream of the transect. The local and instantaneous value of the longitudinal bed shear stress controlling sediment erosion and deposition, as well as the cross-section redistribution of the longitudinal component of the velocity contributing to the discharge, were determined by solving a suitably simplified form of the longitudinal momentum equation, written in curvilinear coordinates and integrated along the normal to the bed (Lundgren and Jonsson 1964). Simulations were carried out in the absence of sea level rise and for a purely erosive scenario, characterized by a negligible external sediment supply to the system. Starting from an initially flat bed with a small incision along the longitudinal axis of the domain a static equilibrium condition was attained asymptotically by both the channel and the adjacent intertidal platform, with the erosive sediment flux vanishing everywhere. The computed equilibrium channel geometry followed the typical power law relationship between channel cross-sectional area and the flowing tidal prism originally developed for tidal inlets (Eq. 10). The simulated channel bed profiles were quite similar to those observed in the Venice Lagoon and tended to collapse on the theoretical relationship derived by Toffolon and Lanzoni (2010) provided that sediment properties, embedded in the choice of the critical velocity for incipient erosion, are appropriately prescribed. The simulated channel funneling was found to be reasonably described by an exponential relationship, even though, for short channels, a linear relationship also provided a good approximation, in accordance with field data from the Venice Lagoon. Low degree of convergence led to an almost linear channel bed profile, while profiles exhibiting and upward concavity were associated with a stronger degree of channel landward convergence. Finally, wider and deeper channels were found to develop as the width of the tidal basin and the tidal amplitude were increased, or the mean intertidal platform elevation was decreased. Narrower and shallower channels were instead generated by increasing the critical shear stress for erosion or decreasing the flow conductance.

3.2 The role of vegetation

The response of the system to vegetation growth depends on the initial conditions, the rate of sea level rise and the presence of wind.

If the channel is initially at (static) equilibrium, with no wind and no sea level rise, it is unable to transport sediments, hence the bed elevation in the channel does not vary except in the narrow drying/wetting region close to

232

Rendiconti Lincei. Scienze Fisiche e Naturali (2022) 33:217–243
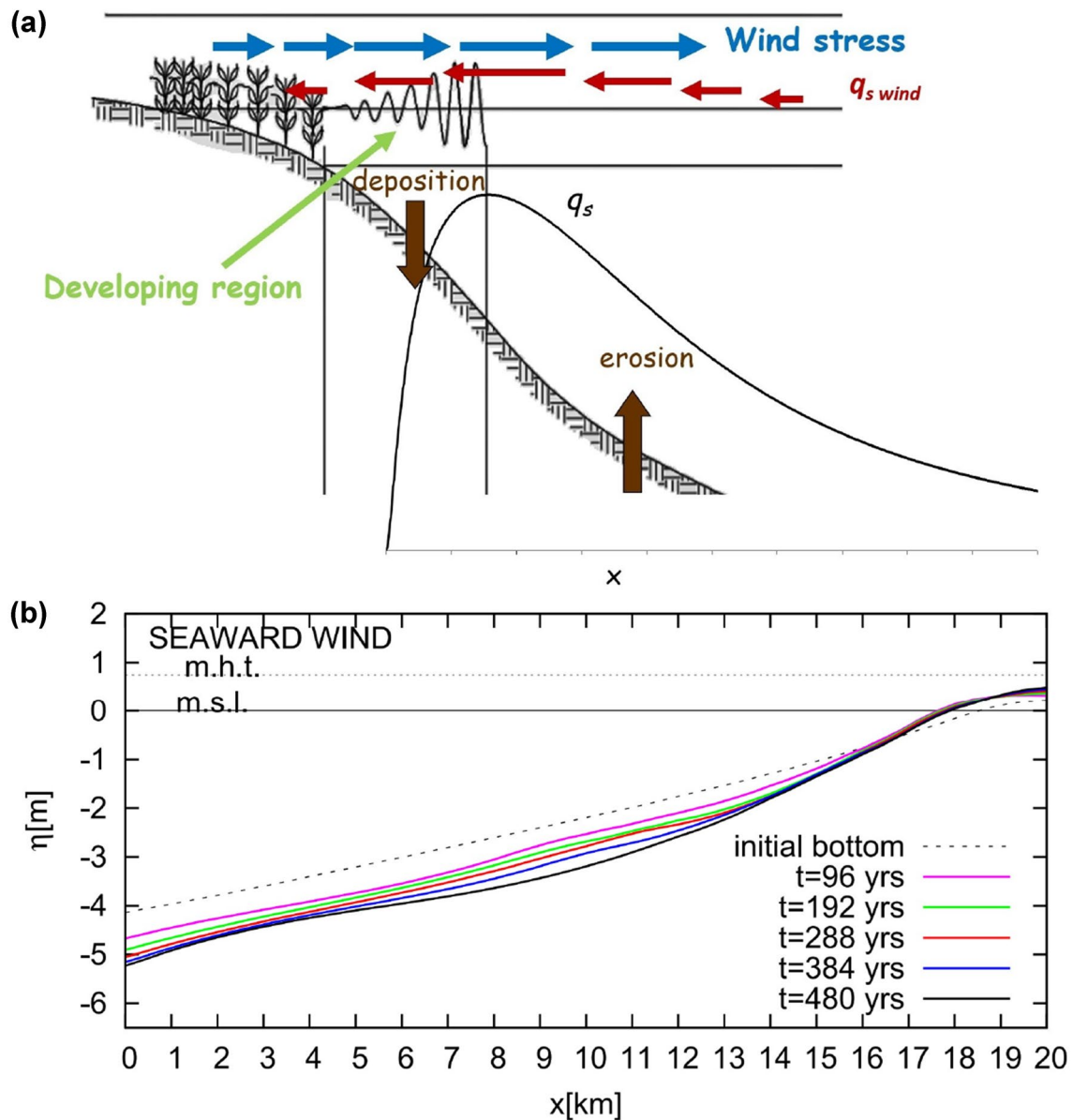
Fig. 15 a Spatial distribution of the maximum shear stress associated with wind waves spatially developing from the marsh border. In addition, plotted is the associated distribution of the sediment flux per unit width and the tendency to deposition (erosion) close to (far from) the marsh border. **b** Evolution of a system channel-flat-unvegetated platform subject to seaward wind (adapted from Tambroni and Seminara 2012)

the marsh margin where the growth of vegetation leads to organic accretion. Accretion also occurs in the marsh, which raises towards mean high tide, until the flow depth has decreased sufficiently to reach the lower limit of biomass productivity such that vegetation disappears. The final state is indeed an equilibrium state, with a fairly steep scarp and no marsh (Fig. 16a). If the initial channel configuration is not in equilibrium, sediments are transported along the channel and deposited on the tidal flat close to the marsh margin where vegetation growth leads to flow deceleration

and reduction of the transport capacity of the stream. The tidal flat accretes and is eventually colonized by vegetation such that the marsh region progra, leaving behind a flat marsh surface which has reached the upper limit for biomass productivity. At the end of the simulation (i.e., after 1000 years), the channel still transported some sediments, hence it was not yet in exact equilibrium (Fig. 16b).

Sea level rise generally threatens salt marsh survival. For a moderate biomass productivity ($B_{max} = 1 \ kg/m^2$) the marsh is unable to keep pace with even a small or moderate rate of

Rendiconti Lincei. Scienze Fisiche e Naturali (2022) 33:217–243

233
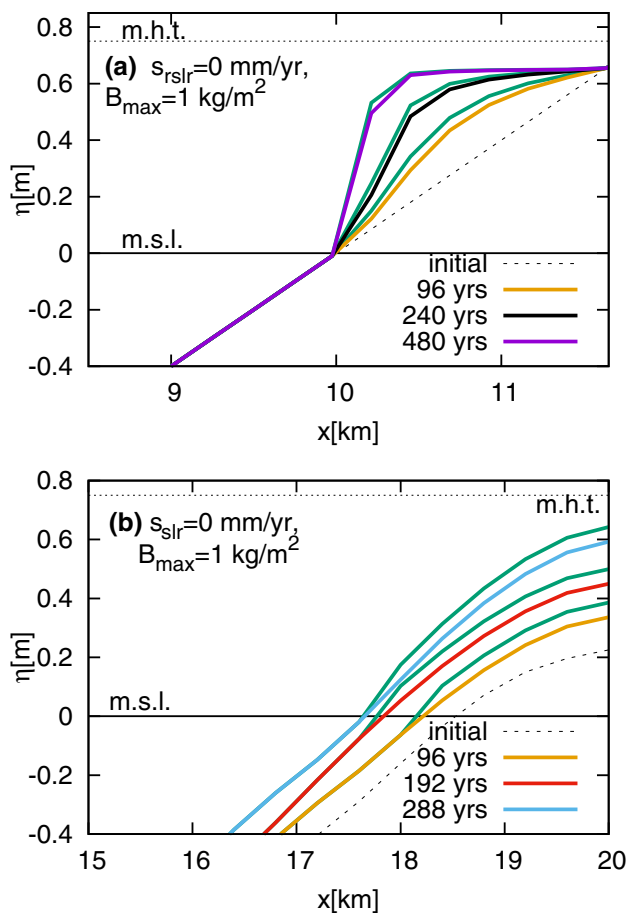
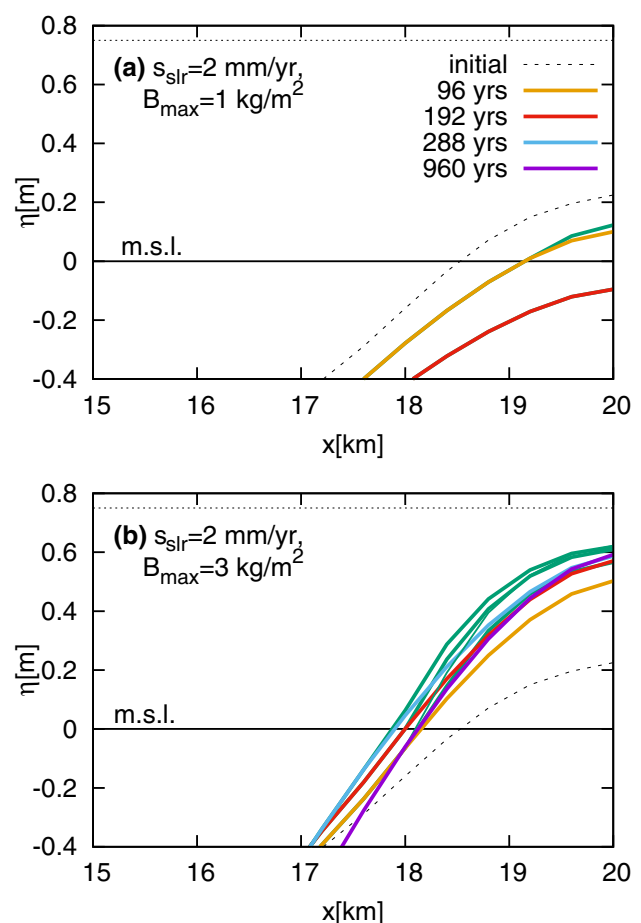**Fig. 16** Temporal evolution of the elevation of the $1-D$ channel-salt marsh system in the absence of sea level rise and wind for simulations starting from an initial configuration of the channel (dashed lines) either at equilibrium (**a**) or out of equilibrium (**b**). B_{max} is the maximum value of biomass density. The vertical distance between green lines and the corresponding bed elevation at a given evolution time (orange, red, black, light blue and purple lines) is proportional to the local biomass density (adapted from Tambroni and Seminara 2012) (color figure online)

Fig. 17 Temporal evolution of the elevation of the $1-D$ channel-saltmarsh system in the presence of sea level rise and in the absence of wind. Simulation started from a channel configuration in non-equilibrium (dashed line). **a** Moderate biomass productivity, $B_{max} = 1$ kg/m^2; **b** high biomass productivity, $B_{max} = 3$ kg/m^2. The vertical distance between green lines and the corresponding bed elevation at a given evolution time (orange, red, light blue and purple lines) is proportional to the local biomass density (adapted from Tambroni and Seminara 2012) (color figure online)

relative sea level rise (e.g., 2 mm/year), with a consequent retreat of salt marsh border and disappearance of vegetation (Fig. 17a). For a sufficiently high biomass productivity ($B_{max} = 3$ kg/m^2), initially the marsh progrades seaward (albeit at a rate slower than in the case of vanishing rate of sea level rise). After roughly 550 years, the salt marsh border slightly retreats and then keeps fixed up to 1000 years. The salt marsh platform rises initially until, after roughly 200 years, it stabilizes at an elevation, relative to mean high tide, lower than that reached in the absence of sea level rise (Fig. 17b). Finally, note that the marsh rate of relative accretion does not vanish everywhere on the marsh at the end of the 1000-year simulations.

If the action of wind is allowed for, the picture changes as a result of the various, previously discussed, processes. Again, close to the marsh border sediment deposition occurs

while erosion occurs further seaward: as a result, the marsh progrades. Second, marsh deposition is more intense than in the tidally dominated case as wind introduces an additional input of mineral sediments. Hence, the marsh profile is flatter than in the tidally dominated case. In addition, sediments resuspended in the tidal flat region are advected by tidal currents over the marsh platform during the flood phase, causing marsh aggradation and eventually the formation of sort of levees close to the marsh border, as sediment deposition is maximum at the marsh edge and decays gradually in the landward direction. Figure 18 shows the results of simulations performed by Tambroni and Seminara (2012) assuming moderate biomass productivity ($B_{max} = 1$ kg/m^2) and two moderate values for the rate of sea level rise (1 mm/year and 2 mm/year).

In general, moderately productive marshes are eventually found to retreat and gradually disappear. The presence of wind, generating deposition close to the marsh margin, leads to initial marsh progradation and slows down the subsequent marsh retreat compared to the no wind case. For a rate of sea level rise of 2 mm/year, the marsh disappears after 320 years (Fig. 19a–c). For a rate of sea level rise of 1 mm/year, the salt marsh manages to survive for 500 years in the no wind case and for 750 years in the case of a landward blowing wind (Fig. 19d–f).

But, if the final fate of most marshes is to disappear, how does the picture emerged from the simulations carried out by Tambroni and Seminara (2012) compare with the prediction of Kirwan et al. (2010) about the existence of a threshold value of the rate of relative sea level rise below which marshes would be stable? To answer the latter question, Tambroni and Seminara (2012) determined the threshold rate of relative sea level rise above which the marsh platform is unable to reach an equilibrium elevation, as a function of the sediment concentration experienced at the channel-marsh boundary for given characteristics of the forcing tide. In other words, the concentration of suspended sediment generated by wind resuspension at the channel-marsh boundary was interpreted as the reference concentration of zero-order models. A comparison of results of $1 - D$ simulations with those of Kirwan et al. (2010) for marshes subject to a 1 m tidal range is fairly satisfactory (Fig. 20a). This apparent contradiction is immediately reconciled observing that the concept of marsh stability in Kirwan et al. (2010) was

associated with the ability of the marsh surface to keep pace with sea level rise, while the concept of marsh equilibrium put forward by Tambroni and Seminara (2012) requires an additional constraint, namely that the channel-marsh boundary does neither prograde nor retreat. Figure 20b shows two examples of $1 - D$ simulations which led to equilibrium states in the sense of Kirwan et al. (2010), where however the marsh boundary did migrate seaward.

It is also worth noting that Mariotti and Fagherazzi (2010), using a different $1 - D$ model, found that, for a given rate of sea level rise and non vanishing sediment concentration at the sea boundary, a unique value of the latter exists such that the marsh boundary does not undergo any horizontal displacement. The $1 - D$ numerical simulations described above show that any possible *equilibrium state* would be unstable as small perturbations would invariably induce migration of the marsh boundary. Further research is definitely needed to explain this discrepancy.

Recently, the mutual effects of tidal currents, sediment availability, sea level rise, and vegetation encroachment on the morphodynamics of a channel-flat system was investigated also by Sgarabotto et al. (2011) who extended the model of Lanzoni and D'Alpaos (2015) presented in Sect. 3.1. The assumption of a quasi-static propagation of the tide was relaxed and wetting/drying effects were accounted for following the approach of Defina (2000). An external sediment supply was introduced within the tidal basin to model the possible aggradation of the intertidal platform flanking the channel and vegetation was allowed to grow when the platform elevation exceeded a given threshold. Wind wave effects were not considered. Model simulations showed that vegetation has two counteracting effects. First, it enhances channel incision and enlargement due to the increase of flow resistance over vegetated areas adjacent to the channel. Second, it strengthens channel infilling and shrinking due to the reduction in tidal prism promoted by vertical marsh accretion. The balance between sea level rise and external sediment availability determines which effect prevails over the other as the system evolves.

Some further information about the eco-morphodynamic coevolution of tidal channels, tidal flats and salt marshes was obtained through the $2 - D$ model developed by Geng et al. (2021). A rectangular tidal basin was taken to mimic tidal environments flanking large tidal channels or tidal rivers. The coevolution was simulated through an eco-morphodynamic model based on a simplified version of the two-dimensional, depth-averaged momentum and mass conservation equations (Van Oyen et al. 2008), on the advection-dispersion equation for suspended sediment concentration and the Exner sediment balance equation. Wind waves effects were not accounted for. Three different biomass distributions depending on bed elevation were used in the simulations (Fig. 21).
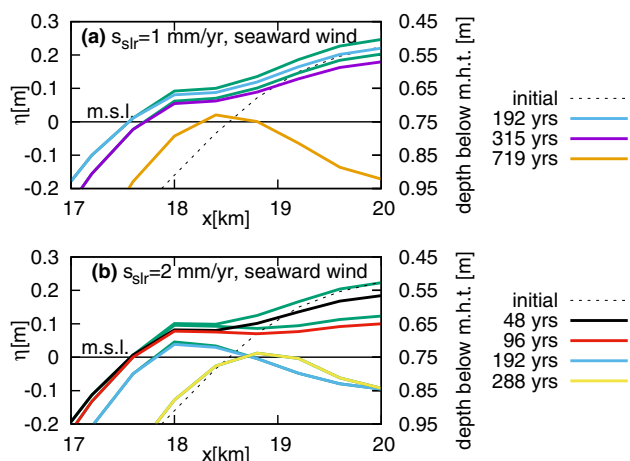
Fig. 18 Temporal evolution of the elevation of the $1 - D$ channel-marsh platform system in the presence of sea level rise and wind. Simulation performed assuming moderate biomass productivity ($B_{max} = 1$ kg/m^2) and two moderate values for the rate of sea level rise. The vertical distance between green lines and the corresponding bed elevation at a given evolution time (black, red, light blue, yellow, purple and orange lines) is proportional to the local biomass density. Simulation started from a channel configuration (dashed line) in non-equilibrium (adapted from Tambroni and Seminara 2012) (color figure online)
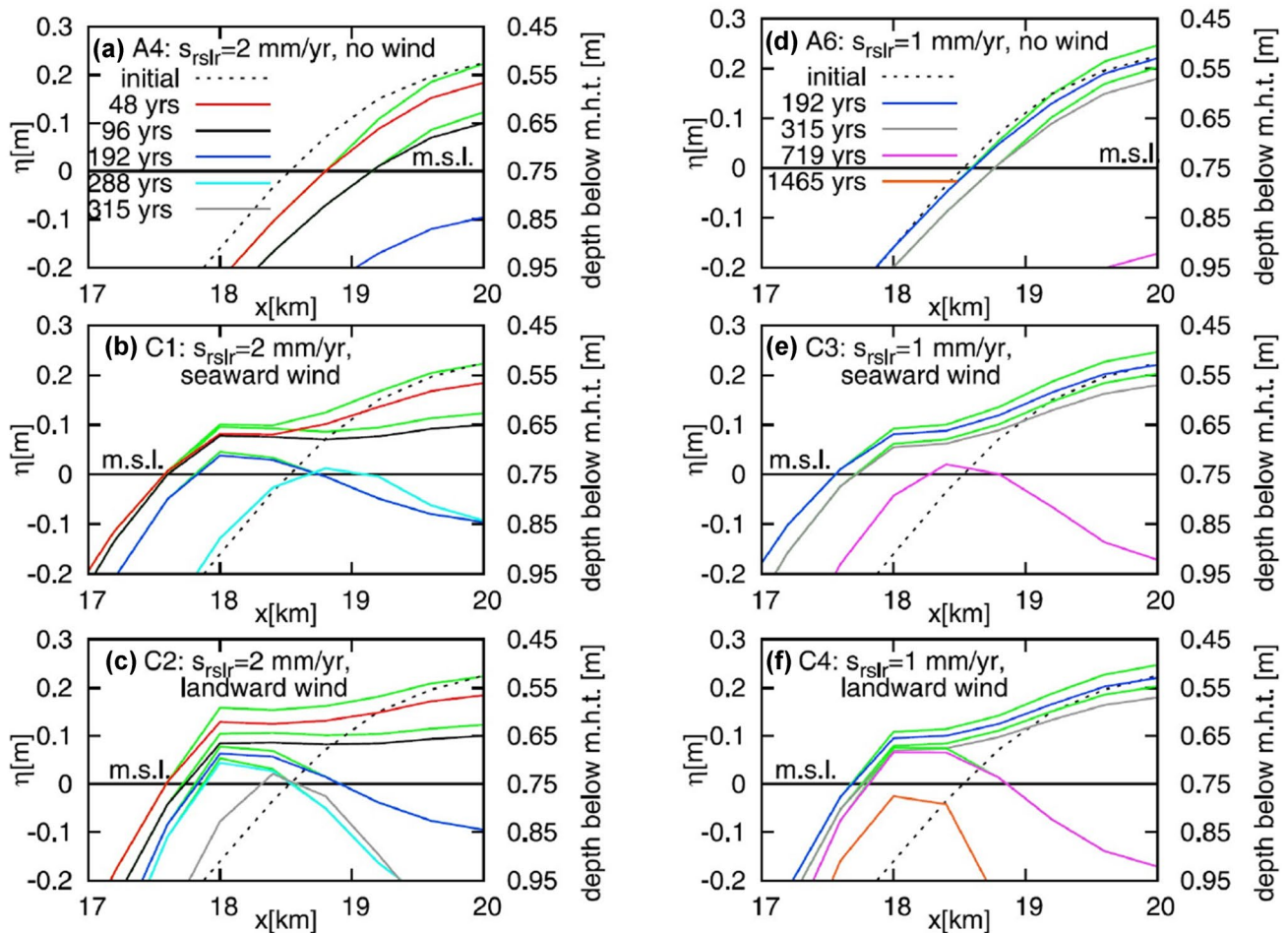
Fig. 19 Long-term evolution of the $1 - D$ marsh profile and vegetation distribution over the marsh showing that the fate of moderately productive marshes ($B_{\max} = 1\ kg/m^2$) is invariably to disappear. The vertical distance between green lines and the corresponding bed elevation at a given evolution time (red, black, blue, light blue, grey, magenta and orange lines) is proportional to the local biomass density. Simulation started from a channel configuration (dashed line) in non-equilibrium (adapted from Tambroni and Seminara 2012) (color figure online)

The tidal system was let evolve starting from a horizontal, slightly and randomly perturbed bed, subject to the forcing of the tide and with a sediment concentration prescribed at the seaward boundary. Model results (Fig. 22) indicate that vegetation with optimal biomass production at an elevation close to MSL enhances the formation of tidal channels. As compared with the bare soil case, channels extend more rapidly landward, getting wider and shallower, generating more branches and, hence, forming more complex networks with a higher drainage efficiency. Vegetation patches started to form near the seaward border, owing to the more rapid accretion of the intertidal platform enforced by the externally supplied sediment concentration. Trapping of suspended sediment by these patches led to a reduction of the amount of sediment delivered to the seaward and middle portions of the basin. There, sedimentation weakened and the extension of salt marsh areas was thus limited. The control of vegetation

on channel morphology reduced in the presence of relative sea level rise. The salt marshes located near the seaward border of the basin were able to keep pace with relative sea level rise only when a sufficient amount of sediment was provided externally. Only a few marshes were able to survive in the inner portion of the basin, with sediment trapping and organic soil production compensating for relative sea level rise. Tidal flats surrounding these isolated marshes were not able to keep pace with the relative sea level rise and, eventually, the tidal basin developed a remarkable landward-decreasing mean bed slope (Fig. 22).

(b)

(a)
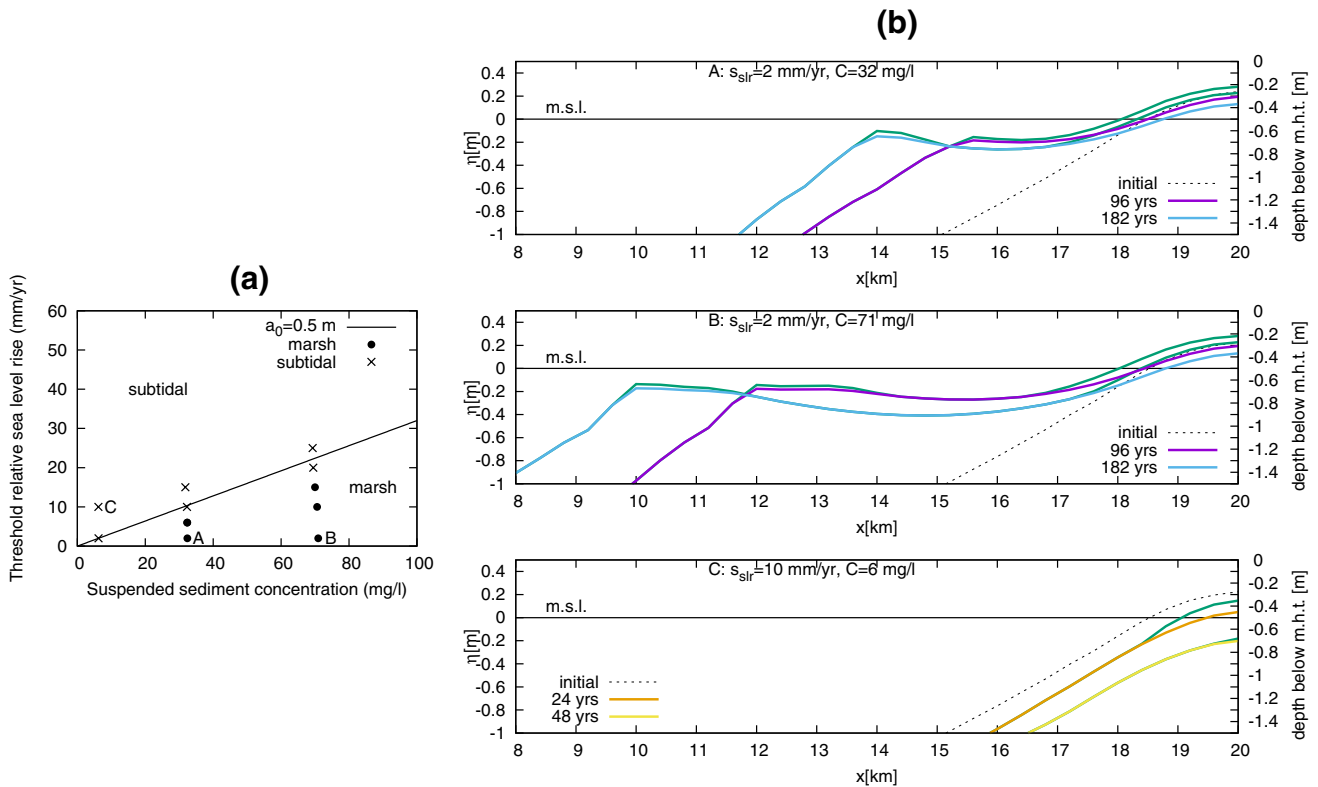
Fig. 20 a Predicted threshold rate of relative sea level rise above which marshes are replaced by sub-tidal environments. The solid line represents the mean threshold rate predicted by Kirwan et al. (2010). Circles denote configurations where the marsh platform was able to reach an equilibrium elevation, while crosses denote cases where the marsh proved unable to keep up with sea level rise and disappeared. **b** Simulations for the three configurations denoted by A, B and C in

a. Note that simulations for the cases A and B, which are equilibrium configurations in the sense of Kirwan et al. (2010), show that the marsh boundary migrates seaward in both cases, with a rate depending on the concentration experienced at the marsh boundary, hence A and B are not in equilibrium in the sense of Tambroni and Seminara (2012)

4 Anthropogenic effects

Results discussed so far refer to transitional environments undergoing a *natural* evolution process. However, many such systems have undergone anthropogenic modifications originated by the exploitation of river basins, sea and wetlands as well as by the effects of human settlements. In the last century, the consequences of such modifications have clearly emerged (Seminara et al. 2011). Let us mention some of them, referring again to Venice lagoon.

4.1 Depleting the fluvial source of sediments for coastal wetlands

A major modification undergone by several transitional environments throughout the world has been a strong cut of the fluvial supply of sediments. In most cases, this has been due to the effects of river regulation and the construction of dammed reservoirs in the upper part of river basins, the most striking example being the Mississippi river. It has been estimated (Meade and Moody 2010) that the sediment supplied
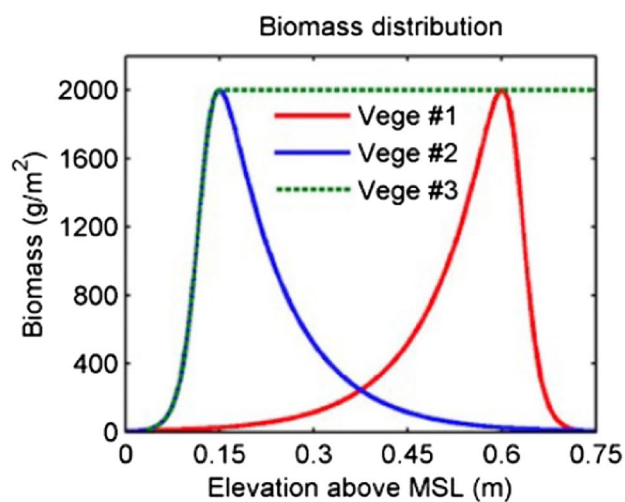
Fig. 21 Biomass distribution as a function of the bed elevation employed by Geng et al. (2021) to mimic three different types of salt-marsh vegetation species

Rendiconti Lincei. Scienze Fisiche e Naturali (2022) 33:217–243

237
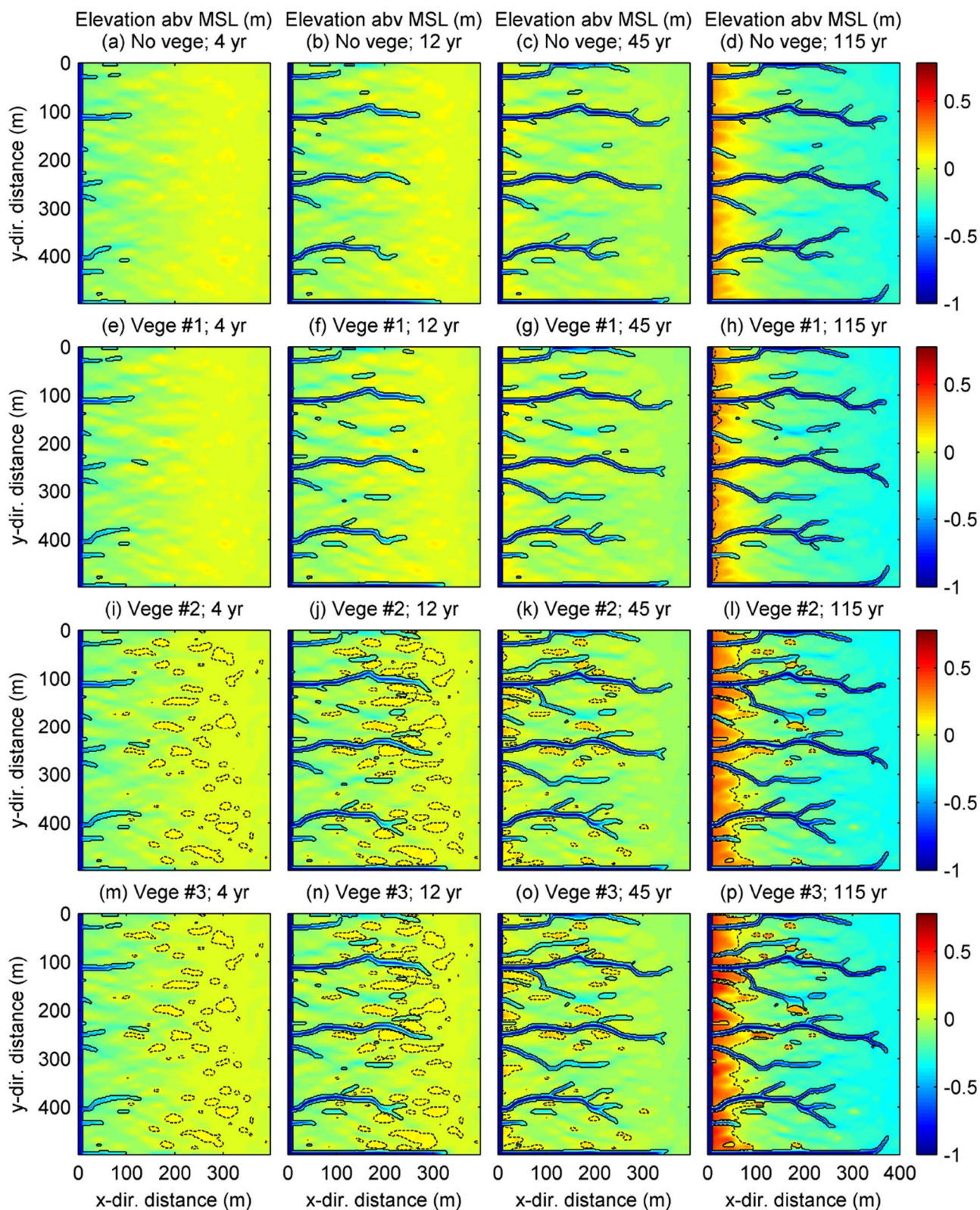
Fig. 22 The spatial distribution of bed elevation (m), referred to mean sea level (MSL), is plotted at different evolution stages (4, 12, 45, and 115 years) for a sea level rise of 4 mm/year. The four simulated cases refer to: bare soil, (**a–d**); Vege #1, (**e–h**); Vege #2, (**i–l**); Vege #3, (**m–** **p**). Black continuous lines denote the edge of tidal channels. Black dashed lines delimit vegetated areas with biomass density larger than 100 g/m². The biomass distribution functions for the three types of vegetation are those shown in Fig. 21 (adapted from Geng et al. 2021)

to the Mississippi delta has nearly halved from 1800 to 1980. Venice lagoon has undergone an even more drastic cut in fluvial supply. All the major rivers debouching into the lagoon were diverted (a long process pursued mostly during the XVI and XVII centuries), to counteract the process of progressive infilling that several areas of the lagoon had been experiencing since the XII century. River diversion has definitely removed the threat of lagoon infilling and reduced health problems as fresh waters generated an environment appropriate to host mosquitos and cause malaria. However, it has also been a major cause of the severe degradation suffered by the lagoon in the following centuries, a slow process which has undergone a sudden acceleration at the beginning of the last century (Fig. 23).

4.2 Modifying the sea-lagoon exchange of sediments

Further anthropogenic modifications were forced to meet the variety of novel requirements prompted by the industrial revolution. Let us illustrate this point referring to our notable example of Venice lagoon.

To allow access of steam ships into the lagoon, jetties were constructed at the inlets, such to narrow them and promote their progressive deepening. These works lasted about one century. Moreover, the decision to locate an industrial hub in Marghera, a town situated at the border of the lagoon, in a period (beginning of the XX century) of rapid industrial development, led to the decision to excavate two large canals, namely the Vittorio Emanuele canal (1920–1925) and the Malamocco-Marghera canal (1964–1968), connecting the Lido and Malamocco inlets to the hub. In particular, the construction of the latter canal (aimed at allowing oil tanks to cross the central lagoon), had a significant impact on the intensity of tidal currents, leading to enhanced export of fine sediments from the lagoon and the consequent deepening of the central lagoon. Finally, land reclamation was pursued (1963–70) to further promote industrial development.

The above interventions influenced the geometry of the inlets, the littoral transport of sediment and the overall amount of sediment which the lagoon exchanges with the sea. In particular, inlets have progressively deepened until they reached a quasi-equilibrium state (Fig. 24). Sediments discharged by the Piave river into the Adriatic sea and transported southward by littoral currents, were intercepted by
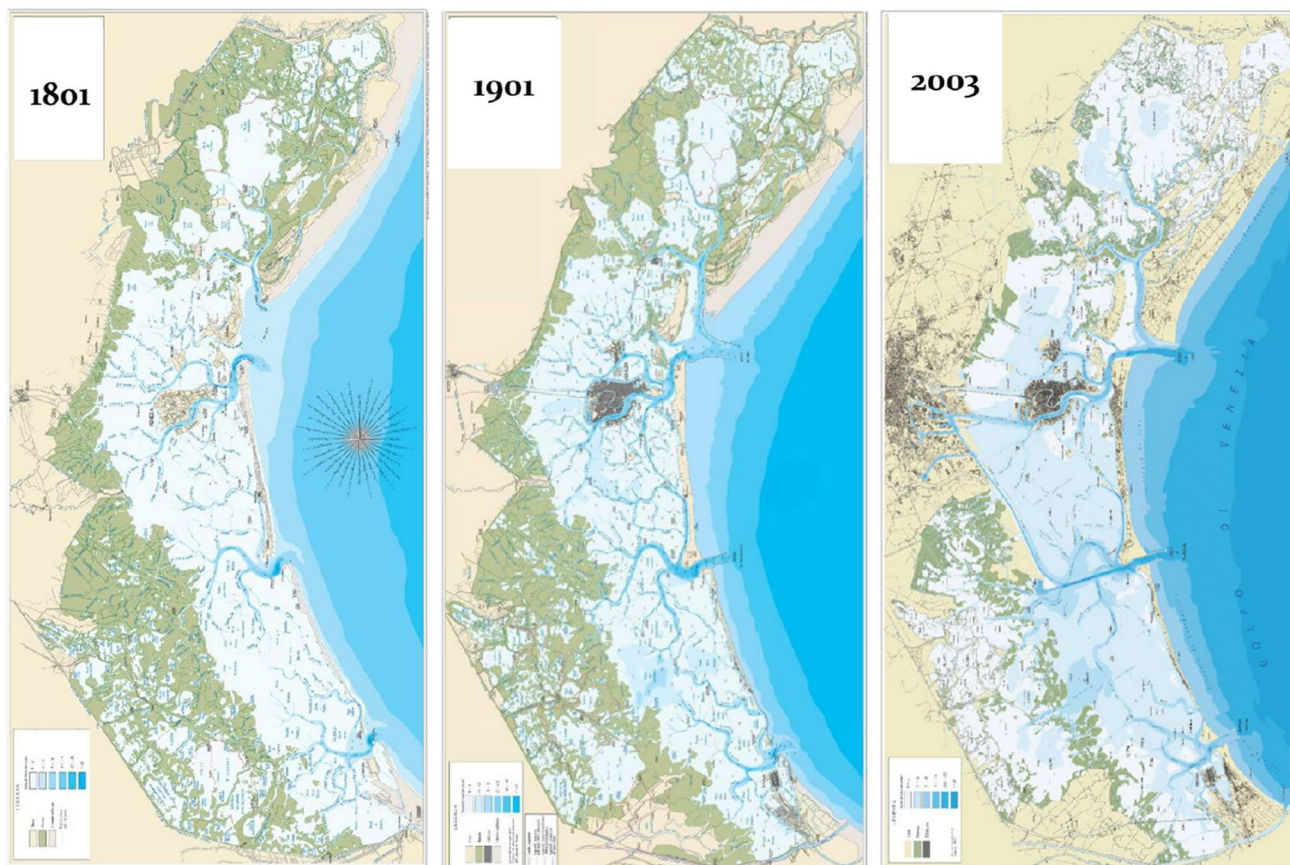
Fig. 23 Maps of Venice lagoon morphology in 1801. 1901 and 2003. Green areas denote salt marshes (courtesy of L. D'Alpaos) (color figure online)

Rendiconti Lincei. Scienze Fisiche e Naturali (2022) 33:217–243

239

Fig. 24 Evolution of the cross-sectional area of each inlet of the Venice Lagoon, starting from the construction of the inlet jetties to the end of the last century (courtesy of Magistrato alle Acque di Venezia)
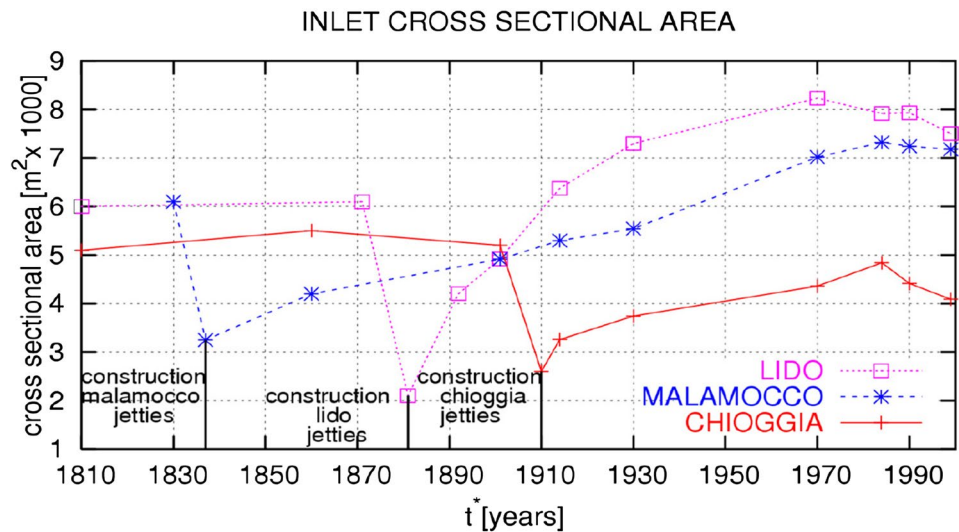
Fig. 25 Sketch illustrating the progradation of the coast north to the Lido inlet of Venice lagoon and the regression south to the same inlet

the northern jetty of the Lido inlet, letting the coast north to the inlet prograde and the southern coast erode (Fig. 25).

Jetties have also induced the channelization of the ebb jet generated at each inlet. As a result, the ebb-flood asymmetry of the flow field in the near inlet region (Blondeaux et al. 1982) was enhanced. Hence, fine sediments, resuspended in sub-tidal and tidal flats during strong wind events and conveyed to the inlets by ebb currents flowing through the tidal network, are now dispersed into the sea far enough from the inlet to be essentially lost for the lagoon. The distance from the inlet reached by the ebb plume is indeed clearly visible in Fig. 25. Moreover, sediment supply to the lagoon originating by resuspension in the surf zone and transported by flood currents has decreased as the inlets have been moved away from the shore (Tambroni et al. 2005). These processes persist nowadays, though the progradation of the coast north to Lido has reestablished a configuration similar to that existing prior to the construction of jetties. Today, the amount of fine sediments lost to the sea through the inlets is estimated in the order of 0.3–0.6 Mm^3 per year and exceed the volume of sand annually imported from the sea which is much lower, roughly 30, 000 m^3 (Magistrato alle Acque di Venezia - Technital 2007; Magistrato alle Acque di Venezia - CORILA 2011).

4.3 Disruption of lagoon environments

Several anthropogenic sources of disruption for the delicate lagoon environment are known. Few examples will suffice.

In Venice lagoon the mechanical devices illegally employed by clam fishermen to *plow* the bottom are known to disrupt the layer of phanerogams which have the major function to protect the lagoon from wind driven erosion. In addition, marsh borders are subjected to *fatigue* effects possibly leading to bank collapse due to the impact of waves

240

Rendiconti Lincei. Scienze Fisiche e Naturali (2022) 33:217–243

generated by ships sailing through the lagoon. Moreover, marsh vegetation may sometimes be removed by anthropogenic perturbations. A striking example has been reported by Kirwan et al. (2008): marshes located in Westham Island, British Columbia, that naturally accrete faster than sea level, have been eroded as a result of geese grazing. Where the latter has been intense, bed elevations have been lowered allowing more rapid wave erosion which has driven the conversion of marshes into mudflats

Anthropogenically induced subsidence is an important process which has enhanced the natural subsidence phenomenon occurring in deltas and coastal lagoons. Anthropogenic subsidence has a variety of sources. In Venice, massive extractions of water from the ground occurred when the Marghera hub was constructed (1950–1970) (Carbognin et al. 2005, Fig. 26). Besides its direct effect on the frequency of high waters, tidal flat deepening affects the height of wind waves and their resuspension capacity. As discussed above (Sect. 2.3), for moderate deepening, flat erosion is enhanced. As deepening increases, the wind induced stress on the flat bottom decreases and tends asymptotically to vanish. Similar, more intense, features have been observed in many coastal areas, most notably along the coast of Louisiana severely affected by the consequences of both coastal and offshore massive extraction of oil (Seminara et al. 2011).

5 Conclusions

Let us summarize our conclusions on the two main issues that motivated our research and are strongly connected to each other: the problem of morphological equilibrium of coastal lagoons and their fate in response to global warming.

Although benefiting from the availability of more powerful computational techniques and an improved quantitative description of the various roles that vegetation plays in marsh morphodynamics, research has not reached a generally agreed conclusion on the issue of marsh equilibrium, as the dichotomy mentioned in our introduction is still somewhat present even in the recent literature. On one hand, the efforts of various groups of researchers (see Kirwan et al. 2010 and Fig. 14) based on zero-order modeling provide a picture suggesting that marsh equilibrium is indeed possible, provided the rate of relative sea level rise does not exceed a threshold depending on the availability of minerogenic sediments, quantified through a somewhat loosely defined sediment concentration C_0. On the other hand, if the morphological interaction between adjacent morphological units is carefully analyzed (Tambroni and Seminara 2012), it turns out that the *equilibrium states* identified by Kirwan et al. (2010) correspond nearly invariably to marshes which either prograde or retreat, i.e., marshes which are not in equilibrium. This is our own viewpoint, supported recently also by the work of Mariotti and Fagherazzi (2010) and Fagherazzi (2013): coastal lagoons are complex environments which are hardly in equilibrium. The timescale of their morphodynamic evolution is, however, of the order of centuries, which makes these processes non easily perceived under ordinary conditions.

In this respect, the case of the Venice Lagoon is paradigmatic. Indeed, in spite of river diversions and of the consequent drastic reduction of the amount of sediments supplied to Venice Lagoon, the process of marsh degradation has proceeded slowly for centuries. However, Fig. 1 suggests that the acceleration of marsh degradation observed in the last few decades will likely proceed and possibly be enhanced as a result of an accelerated sea level rise. Under

Fig. 26 Distinct contributions of sea level rise, natural subsidence and artificial subsidence to the variation of elevation of the Venetian soils during the XX century (after Carbognin et al. 2005)
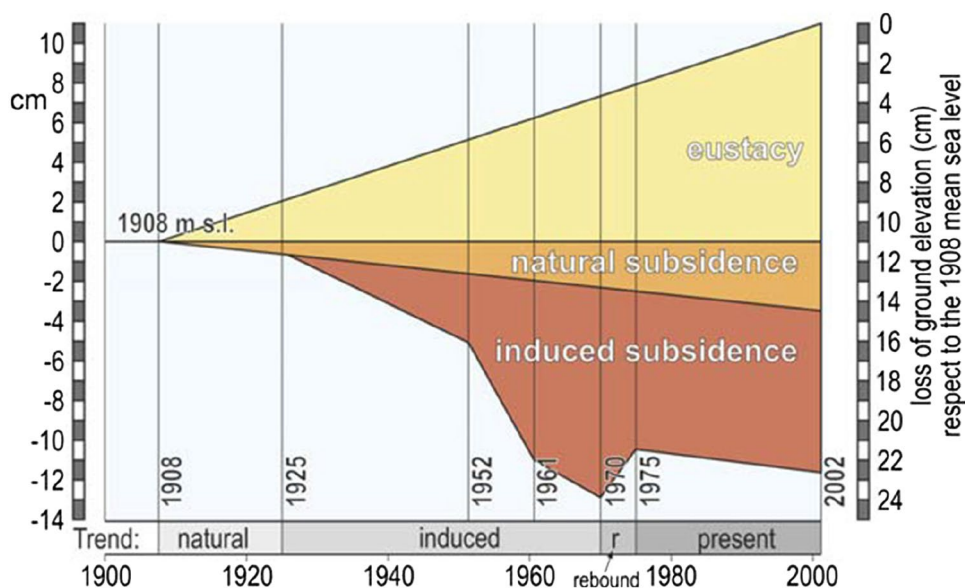
these conditions, the effort required to counteract the clear tendency of Venice Lagoon to evolve towards a bay, will soon become prohibitive. The costly measures undertaken so far, most notably the artificial replenishment of salt marshes, or the suggestion that existing halophytic vegetation might be replaced by more productive species such that organic production may allow wetlands to keep up with sea level rise, will have to be thoroughly revisited. The fate of Venice marshes is strictly tied to the future characteristics that the city of Venice will be forced to attain. But this is another story that will deserve special attention in the future.

References

Magistrato alle Acque di Venezia (2008) Corila C.2.10/IV Aggiornamento del Piano Morfologico. D1: Stato delle componenti naturali e fisiche; stato attuale e tendenze in atto delle componenti idro-morfodinamiche del sistema lagunare. In: Rapporto finale, a cura di IMAGE UniPD. Prodotto dal Concessionario, Consorzio Venezia Nuova **(In Italian)**

Magistrato alle Acque di Venezia Technital (2007) Attività di aggiornamento del piano degli interventi per il recupero morfologico in applicazione della delibera del Consiglio dei Ministri del 15.03.01. In: Studi integrativi. Rapporto finale—Modello morfologico a maglia curvilinea. Relazione di sintesi. Prodotto dal Concessionario Consorzio Venezia Nuova **(In Italian)**

Magistrato alle Acque di Venezia, CORILA (2011) Aggiornamento del piano morfologico della laguna di Venezia. Rapporto finale, Prodotto dal concessionario Consorzio Venezia Nuova **(In Italian)**

Allen JRL (1990) Salt marsh growth and stratification: A numerical model with special reference to the Severn Estuary, Southwest Britain. Mar Geol 95:77–96

Allen JRL (1995) Salt marsh growth and fluctuating sea level: implications of a simulation model for Flandrian coastal stratigraphy and peat-based sea-level curves. Sediment Geol 100:21–45

Blondeaux P, De Bernardinis B, Seminara G (1982) Correnti di marea in prossimità di imboccature e loro influenza sul ricambio lagunare. In: Proceedings of Atti XVIII Convegno Idraulica e Costruzioni Idrauliche, Bologna, 21–23 Sept **(In Italian, English translation available from the Authors)**

Bruun P (1978) Stability of tidal inlets. Elsevier, New York

Cahoon DR, Hensel PF, Spencer T, Reed DJ, McKee KL, Saintilan N (2006) Coastal wetland vulnerability to relative sea-level rise: wetland elevation trends and process controls. In: Verhoeven JTA (ed) Wetlands and natural resource management, ecological studies, vol 190. Springer, New York, pp 271–292

Callaway JC, DeLaune RD, Patrick WH (1997) Sediment accretion rates from four coastal wetlands along the Gulf of Mexico. J Coast Res 13(1):181–191

Carbognin L, Teatini P, Tosi L (2005) Land subsidence in the Venetian area: known and recent aspects. Giornale di Geologia Applicata 1:5–11

Chmura GL, Anisfeld SC, Cahoon DR, Lynch JC (2003) Global carbon sequestration in tidal, saline wetland soils. Global Biogeochem Cycles 17(4):1111. https://doi.org/10.1029/2002GB001917

Christiansen T, Wiberg PL, Milligan TG (2000) Flow and sediment transport on a tidal salt marsh surface. Estuar Coast Shelf Sci 50:315–331

Church JA, White NJ (2006) A 20th century acceleration in global sea-level rise. Geophys Res Lett 33:L01602. https://doi.org/10.1029/2005GL024826

Coco G, Zhou Z, van Maanen B, Olabarrieta M, Tinoco R, Townend I (2013) Morphodynamics of tidal networks: advances and challenges. Mar Geol 346:1–16. https://doi.org/10.1016/j.margeo.2013.08.005

Cronk JK, Fennessy MS (2001) Wetland plants: biology and ecology. Lewis, Boca Raton

D'Alpaos A, Lanzoni S, Mudd SM, Fagherazzi S (2006) Modelling the influence of hydroperiod and vegetation on the cross-sectional formation of tidal channels. Estuar Coast Shelf Sci 69:311–324. https://doi.org/10.1016/j.ecss.2006.05.002

D'Alpaos A, Lanzoni S, Marani M, Rinaldo A (2009) On the O'Brien-Jarrett-Marchi law. Rend Fis Acc Lincei 20:225–236. https://doi.org/10.1007/s12210-009-0052-x

D'Alpaos A, Lanzoni S, Marani M, Rinaldo A (2010) On the tidal prism-channel area relations. J Geophys Res. https://doi.org/10.1029/2008jf001243

Day JW, Templet PH (1989) Consequences of sea level rise: implications from the Mississippi delta. Coast Manag 17:241–257

Day JW, Rybczyk J, Scarton F, Rismondo A, Are D, Cecconi G (1999) Soil accretionary dynamics, sea-level rise and the survival of wetlands in Venice Lagoon: A field and modeling approach. Estuar Coast Shelf Sci 49:607–628. https://doi.org/10.1006/ecss.1999.0522

de Swart HE, Zimmermann JTF (2009) Morphodynamics of tidal inlet systems. Annu Rev Fluid Mech 41:203–229

Defina A (2000) Two-dimensional shallow flow equations for partially dry areas. Water Resour Res 36(11):3251–3264

Defina A, Carniello L, Fagherazzi S, D'Alpaos L (2007) Self-organization of shallow basins in tidal flats and salt marshes. J Geophys Res 112:F03001. https://doi.org/10.1029/2006JF000550

Escoffier FF (1940) The stability of tidal inlets. Shore Beach 8(4):114–115

Exner FM (1925) Über die Wechselwirkung zwischen Wasser und Geschiebe in Flussen, Sitzungsber. Akad Wiss Wien Math Naturwiss Kl Abt 2A 134:165–183

Fagherazzi S (2013) The ephemeral life of a salt marsh. Geology 41:943–944. https://doi.org/10.1130/focus082013.1

Fagherazzi S, Carniello L, D'Alpaos L, Defina A (2006) Critical bifurcation of shallow basin landforms in tidal flats and salt marshes. Proc Natl Acad Sci USA 103:8337–8341. https://doi.org/10.1073/pnas.0508379103 **(ISSN: 0027-8424)**

Fagherazzi S, Palermo C, Rulli M, Carniello L, Defina A (2007) Wind waves in shallow microtidal basins and the dynamic equilibrium of tidal flats. J Geophys Res 112:F02024. https://doi.org/10.1029/2006JF000,572

Fagherazzi S, Kirwan ML, Mudd SM, Guntenspergen GR, Temmerman S, D'Alpaos A, van de Koppel J, Rybczyk JM, Reyes E, Craft C, Clough J (2012) Numerical models of salt marsh

242

Rendiconti Lincei. Scienze Fisiche e Naturali (2022) 33:217–243

evolution: ecological, geomorphic, and climatic factors. Rev Geophys 50:RG1002. https://doi.org/10.1029/2011RG000359

Fredsoe J, Deigaard R (1992) Mechanics of coastal sediment transport. World Scientific Publications, Chennai

French JR (1993) Numerical simulation of vertical marsh growth and adjustment to accelerated sea level rise, North Norfolk. UK. Earth Surf Process Landf 18:63–81

French J (2006) Tidal marsh sedimentation and resilience to environmental change: exploratory modeling of tidal, sea-level, and sediment supply forcing in predominantly allochthonous systems. Mar Geol 235:119–136. https://doi.org/10.1016/j.margeo.2006.10.009

Friedrichs CT (1995) Stability shear stress and equilibrium cross-sectional geometry of sheltered tidal channels. J Coast Res 11(4):1062–1074

Friedrichs CT, Aubrey DG (1996) Uniform bottom shear stress and equilibrium hypsometry of intertidal flats. Mix Estuar Coast Seas Coast Estuar Stud 50:405–429

Friedrichs CT, Perry JE (2001) Tidal salt marsh morphodynamics. J Coast Res 27:6–36

Gehrels WR, Hayward BW, Newnham RM, Southall KE (2008) A 20th century acceleration of sea-level rise in New Zealand. Geophys Res Lett 35:L02717. https://doi.org/10.1029/2007GL032632

Geng L, D'Alpaos A, Sgarabotto A, Gong Z, Lanzoni S (2021) Intertwined eco-morphodynamic evolution of salt marshes and emerging tidal channel networks. Water Resour Res. https://doi.org/10.1029/2021wr030840

Gleason ML, Elmer DA, Pien NC, Fisher JS (1979) Effects of stem density upon sediment retention by salt marsh cord grass, alterniflora Loisel. Estuaries 2(4):271–273. https://doi.org/10.2307/1351574

Gutierrez M, Wangen M (2005) Modeling of compaction and overpressuring in sedimentary basins. Mar Pet Geol 22(3):351–363. https://doi.org/10.1016/j.marpetgeo.2005.01.003

Hughes SA (2002) Equilibrium cross-sectional area at tidal inlets. J Coast Res 18(1):160–174

IPCC (2021) Summary for policymakers. In: Masson-Delmotte V, Zhai P, Pirani A, Connors SL, Péan C, Berger S, Caud N, Chen Y, Goldfarb L, Gomis MI, Huang M, Leitzell K, Lonnoy E, Matthews JBR, Maycock TK, Waterfield T, Yelekci O, Yu R, Zhou B (eds) Climate change 2021: the physical science basis. Contribution of working group I to the sixth assessment report of the Intergovernmental Panel on climate change. Cambridge University Press, Cambridge

Jarrett JT (1976) Tidal prism-inlet area relationships. In: Technical report 3, GITI Report, US Army Engineer Waterways Experiment Station, Vicksburg, MS

Jevrejeva S, Moore JC, Grinsted A, Woodworth PL (2008) Recent global sea level acceleration started over 200 years ago? Geophys Res Lett 35:L08715. https://doi.org/10.1029/2008GL033611

Kearney MS, Rogers AS, Townshend JRG, Rizzo E, Stutzer D, Stevenson JC, Sundborg K (2002) Landsat imagery shows decline of coastal marshes in Chesapeake and Delaware Bays. Eos Trans AGU 83(16):173–178. https://doi.org/10.1029/2002EO000112

Kirwan ML, Murray AB, Boyd WS (2008) Temporary vegetation disturbance as an explanation for permanent loss of tidal wetlands. Geophys Res Lett 35:L05403. https://doi.org/10.1029/2007GL032681

Kirwan ML, Guntenspergen GR, D'Alpaos A, Morris JT, Mudd SM, Temmerman S (2010) Limits on the adaptability of coastal marshes to rising sea level. Geophys Res Lett 37:L23401. https://doi.org/10.1029/2010GL045489

Kjerfve B (1994) Coastal lagoons, chapter 1. In: Kjerfve B (ed) Coastal Lagoon processes, Elsevier Oceanographical Series 60. Elsevier Science Publishers, Amsterdam

Krishnamurthy M (1977) Tidal Prism of Equilibrium Inlets. J Waterw Port Coast Ocean Division 103(4):423–432. https://doi.org/10.1061/JWPCDX.0000051

Krone RB (1987) A method for simulating historic marsh elevations. In: Kraus NC (ed) Coastal sediments '87. American Society of Civil Engineering, New York, pp 316–323

Lambeck K (2021) For the security of coastal communities, to what extent can we trust the available projections of future sea-level rise? In: Report on the Current Issues in Climate Research Conference, Accademia dei Lincei, Rome, pp 20–21. 9-10 September 2021. https://www.lincei.it/sites/default/files/2377_Climate_Report_final_version_31.08.21_1.pdf

Lanzoni S, D'Alpaos A (2015) Earth surface on funneling of tidal channels. J Geophys Res F Earth Surf 120:433–452. https://doi.org/10.1002/2014JF003203

Lanzoni S, Seminara G (2002) Long-term evolution and morphodynamic equilibrium of tidal channels. J Geophys Res 107(C1):3001. https://doi.org/10.1029/2000JC000468

Le Hir P, Monbet Y, Orvain F (2007) Sediment erodability in sediment transport modelling: can we account for biota effects? Cont Shelf Res 27:1116–1142. https://doi.org/10.1016/j.csr.2005.11.016

Leonard LA, Croft AL (2006) The effect of standing biomass on flow velocity and turbulence in Spartina alterniflora canopies. Estuar Coast Shelf Sci 69(3–4):325–336. https://doi.org/10.1016/j.ecss.2006.05.004

Leonard LA, Luther ME (1995) Flow hydrodynamics in tidal marsh canopies. Limnol Oceanogr 40(8):1474–1484. https://doi.org/10.4319/lo.1995.40.8.1474

Levins R (1969) Some demographic and genetic consequences of environmental heterogeneity for biological control. Bull Entomol Soc Am 15:237–240

Lundgren H, Jonsson I (1964) Shear and velocity distribution in shallow channels. J Hydraul Eng Div 90(1):1–21

Marani M, Lanzoni S, Zandolin D, Seminara G, Rinaldo A (2002) Tidal meanders. Water Resour Res 38(11):1225–1231. https://doi.org/10.1029/2001WR000404

Marani M, D'Alpaos A, Lanzoni S, Carniello L, Rinaldo A (2007) Biologically controlled multiple equilibria of tidal landforms and the fate of the Venice lagoon. Geophys Res Lett 34:L11402. https://doi.org/10.1029/2007GL030178

Marani M, D'Alpaos A, Lanzoni S, Carniello L, Rinaldo A (2010) The importance of being coupled: Stable states and catastrophic shifts in tidal biomorphodynamics. J Geophys Res 115:F04004. https://doi.org/10.1029/2009JF001600

Marchi E (1990) Sulla stabilità delle bocche lagunari a marea. Rend Fis Acc Lincei 1:137–150. https://doi.org/10.1007/BF03001888

Mariotti G, Fagherazzi S (2010) A numerical model for the coupled long-term evolution of salt marshes and tidal flats. J Geophys Res 115:F01004. https://doi.org/10.1029/2009JF001326

Mariotti G, Fagherazzi S (2012) Channels-tidal flat sediment exchange: the channel spillover mechanism. J Geophys Res 117:C03032. https://doi.org/10.1029/2011JC007378

Meade RH, Moody JA (2010) Causes for the decline of suspended-sediment discharge in the Mississippi River system, 1940–2007. Hydrol Process 24:35–49. https://doi.org/10.1002/hyp.7477

Milliman JD, Broadus JM, Gable F (1989) Environmental and economic implications of rising sea level and subsidence deltas: The Nile and Bengal examples. AMBIO 18:340–345

Morris JT, Sundareshwar PV, Nietch CT, Kjerfve B, Cahoon DRE (2002) Responses of coastal wetlands to rising sea level. Ecology 83:2869–2877

Mudd SM, Fagherazzi S, Morris JT, Furbish DJ (2004) Flow, sedimentation, and biomass production on a vegetated salt marsh in South Carolina: toward a predictive model of marsh morphologic and ecologic evolution. In: Fagherazzi S, Marani M, Blum LK (eds)

The ecogeomorphology of salt marshes, coastal and estuarine studies, vol 59. AGU, Washigton, pp 165–188

Mudd SM, Howell SM, Morris JT (2009) Impact of dynamic feedbacks between sedimentation, sea-level rise, and biomass production on near surface marsh stratigraphy and carbon accumulation. Estuar Coast Shelf Sci 82(3):377–389. https://doi.org/10.1016/j.ecss.2009.01.028

Mudd SM, D'Alpaos A, Morris JT (2010) How does vegetation affect sedimentation on tidal marshes? Investigating particle capture and hydrodynamic controls on biologically mediated sedimentation. J Geophys Res 115:F03029. https://doi.org/10.1029/2009JF001566

Nepf H (1999) Drag, turbulence and diffusivity in flow through emergent vegetation. Water Resour Res 35(2):479–489

Neumeier U (2007) Velocity and turbulence variations at the edge of saltmarshes. Cont Shelf Res 27(8):1046–1059. https://doi.org/10.1016/j.csr.2005.07.009

Nyman JA, Walters RJ, Delaune RD, Patrick WH (2006) Marsh vertical accretion via vegetative growth. Estuar Coast Shelf Sci 69(3–4):370–380. https://doi.org/10.1016/j.ecss.2006.05.041

O'Brien MP (1931) Estuary tidal prisms related to entrance areas. Civ Eng 1(8):738–739

O'Brien MP (1969) Equilibrium flow areas of inlets on sandy coasts. J Waterw Harb Div ASCE 95:43–52

Randerson PF (1979) A simulation model of salt-marsh development and plant ecology. In: Knights B, Phillips AJ (eds) Estuarine and coastal land reclamation and water storage. Saxon House, Farnborough, pp 48–67

Redfield AC (1965) Ontogeny of a salt marsh estuary. Science 147:50–55. https://doi.org/10.1126/science.147.3653.50

Reed DJ (1995) The response of coastal marshes to sea-level rise: survival or submergence? Earth Surf Process Landf 20:39–48. https://doi.org/10.1002/esp.3290200105

Schuttelaars HM, de Swart HE (1996) An idealized long-term morphodynamic model of a tidal embayment. Eur J Mech B Fluids 15:55–80

Schuttelaars HM, de Swart HE (2000) Multiple morphodynamic equilibria in tidal embayments. J Geophys Res Oceans 105(C10):24105–24118. https://doi.org/10.1029/2000JC900110

Seminara G, Lanzoni S, Solari L, Bolla Pittaluga M (2001) Estuarine patterns: an introduction to their morphology and mechanics. In: Balmforth NJ, Provenzale A (eds) Geomorphological fluid mechanics, lecture notes in physics. Springer, Berlin, pp 455–499

Seminara G, Lanzoni S, Tambroni N, Toffolon M (2010) How long are tidal channels? J Fluid Mech 643:479–494

Seminara G, Lanzoni S, Cecconi G (2011) Coastal wetlands at risk: learning from Venice and New Orleans. Ecohydrol Hydrobiol 11(3–4):183–202. https://doi.org/10.2478/v10104-011-0040-5

Sgarabotto A, D'Alpaos A, Lanzoni S (2021) Effects of vegetation, sediment supply and sea level rise on the morphodynamic evolution of tidal channels. Water Resour Res. https://doi.org/10.1029/2020wr028577

Silvestri S, Defina A, Marani M (2005) Tidal regime, salinity and salt marsh plant zonation. Estuar Coast Shelf Sci 62(1–2):119–130. https://doi.org/10.1016/j.ecss.2004.08.010

Stevenson JC, Ward LG, Kearney MS (1986) Vertical accretion in marshes with varying rates of sea-level rise. In: Wolfe DA (ed) Estuarine variability. Academic Publisher, Orlando, pp 241–259

Swenson EM, Swarzenski CM (1995) Water levels and salinity in the Barataria-Terrebonne estuarine system. In: Reed DJ (ed) Status and historical trends of hydrologic modification, reduction in sediment availability, and habitat loss/modification in the Barataria and Terrebonne estuarine systems, vol 20. Barataria-Terrebonne National Estuary Program, Thibodaux, pp 129–201

Tambroni N, Bolla Pittaluga M, Seminara G (2005) Laboratory observations of the morphodynamic evolution of tidal channels and tidal inlets. J Geophys Res 110:F04009. https://doi.org/10.1029/2004JF000243

Tambroni N, Seminara G (2009) On the theoretical basis of O'Brien-Jarret-Marchi law for tidal inlets and tidal channels. In: Vionnet M, Garcia H, Latrubesse EM, Perillo GME (eds) Proceedings of the 6th IAHR symposium on river, coastal and Eestuarine morphodynamics, 21–25 September 2009, Santa Fe, Argentina, C. A. 1, pp 329–335, Taylor and Francis/Balkema

Tambroni N, Seminara G (2012) A one-dimensional eco-geomorphic model of marsh response to sea level rise: Wind effects, dynamics of the marsh border and equilibrium. J Geophys Res 117:F03026. https://doi.org/10.1029/2012JF002363

Todeschini I, Toffolon M, Tubino M (2008) Long-term morphological evolution of funnelshape tide-dominated estuaries. J Geophys Res 113:C5. https://doi.org/10.1029/2007JC004094

Toffolon M, Lanzoni S (2010) Morphological equilibrium of short channels dissecting the tidal flats of coastal lagoons. J Geophys Res 115:F04036. https://doi.org/10.1029/2010JF001673

van der Wal D, Pye K (2004) Patterns, rates, and possible causes of salt marsh erosion in the Greater Thames area (UK). Geomorphology 61(3–4):373–391. https://doi.org/10.1016/j.geomorph.2004.02.005

van der Wegen M, Wang ZB, Savenije HHG, Roelvink JA (2008) Long-term morphodynamic evolution and energy dissipation in a coastal plain, tidal embayment. J Geophys Res 113:F03001. https://doi.org/10.1029/2007JF000898

Van Oyen T, Carniello L, D'Alpaos A, Temmerman S, Troch P, Lanzoni S (2016) An approximate solution to the flow field on vegetated intertidal platforms: applicability and limitations. J Geophys Res Earth Surf 119:419–433. https://doi.org/10.1002/2016JF004033

Yang SL, Li H, Ysebaert T, Bouma TJ, Zhang WX, Wang Y, Li P, Li M, Ding P (2008) Spatial and temporal variations in sediment grain size in tidal wetlands, Yangtze Delta: on the role of physical and biotic controls. Estuar Coast Shelf Sci 77(4):657–671. https://doi.org/10.1016/j.ecss.2007.10.024

Young IR, Verhagen LA (1996) The growth of fetch limited waves in water of finite depth. Part I: total energy and peak frequency. Coast Eng 28:47–78

Zhou Z, Coco G, Townend I, Olabarrieta M, van der Wegen M, Gong Z, Zhang C (2017) Is "Morphodynamic Equilibrium'' an oxymoron? Earth Sci Rev 165:257–267. https://doi.org/10.1016/j.earscirev.2016.12.002